# SSB transmitter design for 20 m band

Study of filter method SSB transmitter development

Author: SP6GK, 2022

This is my engineering thesis written in 2022 which I have defended in 2023.

# Contents

**1 Theoretical background and goals** **2**
1.1 SSB theory, methods of generation . . . 2
1.2 Goals and constraints . . . 3
1.3 Theory of operation . . . 4

**2 Implementation of stages** **5**
2.1 Audio frequency . . . 5
2.2 Local oscillator . . . 7
2.3 DSB generator . . . 8
2.3.1 Double balanced mixer . . . 8
2.3.2 NE602 . . . 8
2.3.3 MC1496 . . . 9
2.4 SSB filter . . . 10
2.4.1 Crystal parameters . . . 10
2.4.2 Crystal ladder filter . . . 11
2.4.3 Filter components calculation and simulation . . . 14
2.4.4 Real filter construction and impedance matching . . . 16
2.5 VFO . . . 18
2.5.1 Theory of DDS . . . 18
2.5.2 Implementation of DDS . . . 18
2.5.3 Transmit mixer . . . 21
2.5.4 Output band pass filter design and evaluation . . . 22
2.6 Test with the receiver . . . 24
2.7 Linear amplifier . . . 25
2.7.1 Pre-amplifier . . . 25
2.7.2 Final stage . . . 28
2.7.3 Low pass filter . . . 30
2.7.4 Output measurements . . . 31

**3 Mechanical design** **34**
3.1 PCB . . . 34
3.2 Case . . . 35

**4 Conclusions** **36**

# Abstract

Over the recent years a steady technological progress in the digital domain has allowed engineers and radio experimenters to implement cheap and efficient software defined radios (SDRs) for amateur and professional use. Now more than ever radio enthusiasts have access to high grade measurement instruments and good reference receivers. Market presence of still produced analog parts that were designed for nowadays relatively low frequencies poses a great opportunity for a study of an analog transmitter design.

Single Side Band (SSB) is an efficient form of analog modulation which is the most present form of modulation on shortwave bands when it comes to amateur voice transmissions. Many DIY designs of SSB transmitters have been presented by the experimenters, some of them even achieved wide recognition among the amateur radio operators such as Elecraft[4]. However many published designs don't go in depth when it comes to spectrum measurements, sideband rejection, IMD products or they don't specify tuning procedures of vital RF stages for best selectivity.

**Goal of this thesis is to design from scratch a single sideband transmitter for 20 m band (14 MHz) with simulation of stages, validation measurements and baseline calculations**. Created design presents a filter method of SSB generation. Simple audio compression method will be analyzed. Comparison between two popular balanced mixers will be presented. In depth measurement and calculations based on two different methods for a crystal ladder SSB filter will be conducted. DDS variable frequency oscillator implementation will be shown as one of the examples of mixing the analog and digital domain. At the end a non ordinary way of using a power MOSFET will be shown in a linear RF power amplifier.

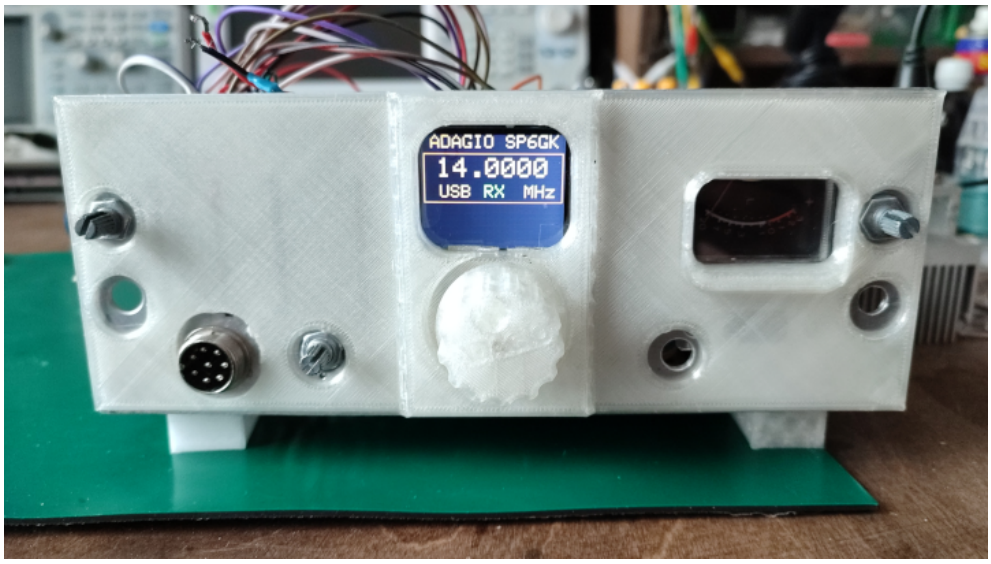


Figure 1: Designed transmitter

# Chapter 1

# Theoretical background and goals

## 1.1 SSB theory, methods of generation

Single side band is an efficient modulation scheme for voice communication. The first method of carrying the voice over a radio, the amplitude modulation (AM) is simple to create using any non linear component. However the AM has some significant disadvantages. It has two side bands that contain identical information. This makes it not only inefficient because it uses twice the spectrum bandwidth necessary but also because it spreads the power across two symmetrical side bands. Furthermore the AM puts about $\frac{1}{3}$ of the transmit power into the carrier which contains no information.

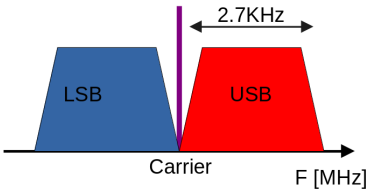


Figure 1.1: Example of AM modulation

Overall for AM (A3E class of emission by ITU[10]) $\frac{1}{3}$ of the power goes into the carrier and $\frac{2}{3}$ goes into sidebands which contain the same information in symmetrical way. This means that efficiency of the AM system is limited to 33%, this is reflected in the modulation depth of AM. Efficiency can be improved by carrier suppression.
SSB goes further in improvements by rejecting one of the sideband and attenuating the carrier. Meaning that all the original information is still transmitted with lower bandwidth required and higher power density in the spectrum. Single sideband suppressed carrier discussed in this thesis is also known as J3E by ITU designation[10].

Two major methods of SSB creation in analog system can be distinguished:

### Phasing method

In this method the modulating signal is split into two mixers. One signal path goes through Hilbert transformation (is shifted by $\pm 90°$). Local oscillator is also split into two mixers with one path shifted by $\pm 90°$). Both mixers are balanced and they provide strong attenuation of the carrier. Output from the mixers is either summed or subtracted to create USB or LSB[7].
Block diagram is presented in fig. 1.2.

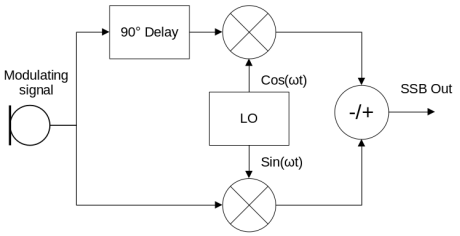


Figure 1.2: Block diagram of phase method

An example of a transceiver using such RF chain was published by Andrzej Janeczek, SP5AHT in July of 2009 in "Elektronika" magazine[12]. This device was published as a kit by AVT and author of the article provides graph showing the re-

sponse of the output from the SSB exciter.

In hardware implementation this method requires two phase shifters, construction of which is not easy and off the shelf solutions are either pricey or they take a lot of space. From the response of the circuit shown by SP5AHT it is visible that attenuation of unwanted sideband depends on how well the modulating phase shifting networks keep the constant angle across the whole modulating frequency spectrum. Non constant phase shift causes ripple at some frequencies resulting in poor sideband rejection.

**Filter method**

This method uses a single balanced mixer in comparison to two used in the phasing method. This mixer creates a double sideband signal with an attenuated carrier. This signal is then passed by a band pass filter which passes one sideband and rejects the other. This method can provide good results but requires very steep and narrow filter for good selectivity. Chain of this method is presented in fig. 1.3.

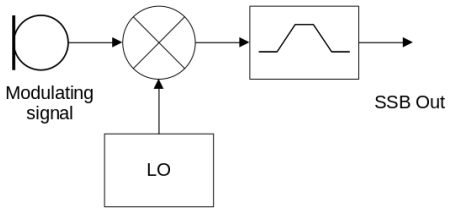


Figure 1.3: Block diagram of filter method

One of the most popular and successful kit in the amateur radio uses this method. Elecraft is an American company based in California that sells kits and ready ham radio products since 1998. Their recent transceiver K3S uses 6 crystal ladder filter proving the effectiveness of this method[4].

This method was chosen over phasing method because it gives more consistent attenuation across the stop band and is overall more popular in hardware based solutions.

Example of a SSB modulation in spectrum domain is shown in fig. 1.4. One has to remember that perfect attenuation of a signal is usually not possible and that some margin of tolerance should be assumed. The Goal of carrier suppression and sideband rejection will be presented in section 1.2

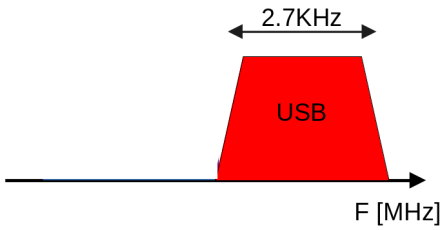


Figure 1.4: Ideal case of SSB modulation

## 1.2 Goals and constraints

Main goal of this work is to create a single side band exciter with linear RF amplifier. Desired output power is to be more than 10 Watts into 50 Ω load with SFDR of at least 40 dB. Transmitter should produce similar amount of power across the whole 20 m band which spans from 14 MHz to 14.35 MHz. Bandwidth of the transmission should be less than 3 KHz. Demodulated voice signal from the transmitter should be understandable on the receiving end.

The audio-frequency bandwidth (-3 dB) of the transmitter should not exceed 3 KHz and 2.7 KHz bandwidth will be a goal. Attenuation slope should be at least 35 dB/KHz with lower frequencies attenuated at a rate of 6 dB/octave[8].

Carrier suppression should be better than 30 dB and unwanted side band rejection should exceed 30 dB. According to FCC the mean power of spurious emission must be at least 43 dB below the mean power of fundamental transmission[9].
Transmitter should also display the frequency with resolution of 10 Hz and transmission should not be possible while the indicated frequency is out of band.

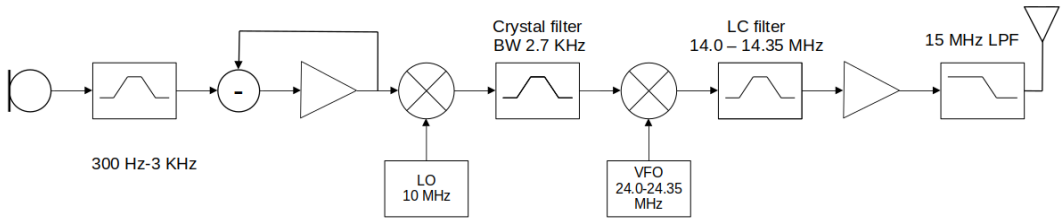


Figure 1.5: Block diagram of transmitter

## 1.3 Theory of operation

### Audio input

Input to the transmitter is a condenser microphone. Audio-frequency signal passes through an LC band pass filter and is then amplified. Audio-frequency passband of -3 dB for this transmitter will be 300 Hz - 3 kHz which is enough of channel to carry a human voice.
Microphone preamplifier is cascaded with a band pass filter to limit spectral bandwidth of double sideband signal generated by following balanced mixer.

### Audio Compressor

Compression limits the dynamic range by application of higher amplification to quiet sounds and decrease in amplification to louder sounds. This naturally introduces some level of distortion, however adequate level of audio compression increases performance of SSB transmitter by improving a signal to noise ratio (SNR) at the receiving end[5]. In fig. 1.5 an audio compressor can be seen as an amplifier with a feedback loop and a sum. Part of the input signal is subtracted by a value proportional to the amplitude of the output. Hence decreasing gain for increasing input amplitude.

### DSB generation, first mixer

Audio-frequency signal of proper level goes then to a double balanced mixer which uses a local oscillator with constant frequency to create a double sideband with suppressed carrier. This is a significant step for carrier suppression. Single frequency LO is used because it allows for creation of filter that can operate on one frequency.

### SSB generation

DSB signal is then passed through a narrow filter which rejects unwanted sideband. SSB filter not only rejects unwanted sideband generating actual SSB, it also adds additional carrier attenuation because low frequency of the filter should be set 300 Hz apart from the carrier. This increases carrier attenuation by more than 10 dB if the filter meets the ITU recommendations mentioned in section 1.2.

### VFO, second mixer

Created SSB signal needs to be shifted to a proper transmit frequency this is done with a mixer. Mixer creates the sum and difference of two frequencies, the desired SSB signal and sinusoidal signal from the variable frequency oscillator (VFO). Output from the second mixer needs to pass through a band pass filter in order to remove the local oscillator signal and other spurious signals.

### Amplifier

SSB signal at proper frequency needs then to be amplified and fed to the antenna. Amplifier needs to be very linear in order not to introduce new spurious signals. In order for clean output and low harmonics a low pass filter is also used.

# Chapter 2

# Implementation of stages

## 2.1 Audio frequency

The AF section consists of two main blocks, the microphone amplifier and compressor. Compressor can be treated as a variable gain amplifier. Option to switch off the compressor is available making it just another constant gain amplifier.

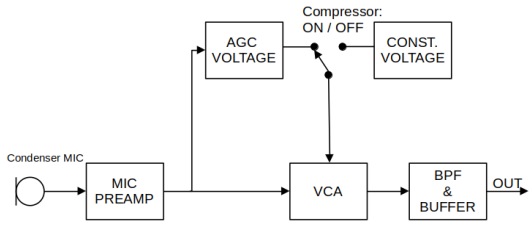


Figure 2.1: Block diagram of AF section

### Microphone amplifier

Condenser microphone is connected between a 4.7k resistor and DC rail to an LC band pass filter. This signal is then amplified by an inverting amplifier with variable gain thanks to a potentiometer in feedback loop. Operational amplifier operates from a single rail thanks to a voltage divider connected to a non-inverting input. This half of positive DC rail voltage needs to be well decoupled in order to prevent oscillations[14]. Schematic of this stage is shown in fig. 2.5. Voltage gain of 5 is sufficient for this stage. NE5532 was chosen for the audio purpose because of its wide unity gain bandwidth. It is worth to remember that with higher gain the bandwidth of the operational amplifier decreases.

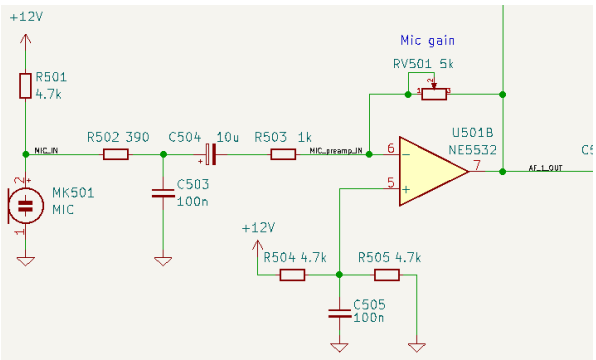


Figure 2.2: Microphone amplifier

### Audio compressor

Audio compressor uses two operational amplifiers. One is applying a significant amplification to a signal coming from a microphone amplifier. This signal with high amplitude is then rectified with a signal diode and smoothed with a capacitor creating a DC voltage that is proportional to amplitude of incoming audio signal. This DC level serves as a control voltage to control gain of second stage amplifier.

Second op amp serves as a voltage controlled amplifier (VCA). This is realized by the use of P-channel JFET before the inverting input instead of constant resistor. JFET changes its resistance as the DC control voltage is applied to it creating a ratio with a feedback resistor which controls the gain of a stage. Control voltage can also be switched to a constant voltage from a voltage divider which in effect turns off the compression effect.

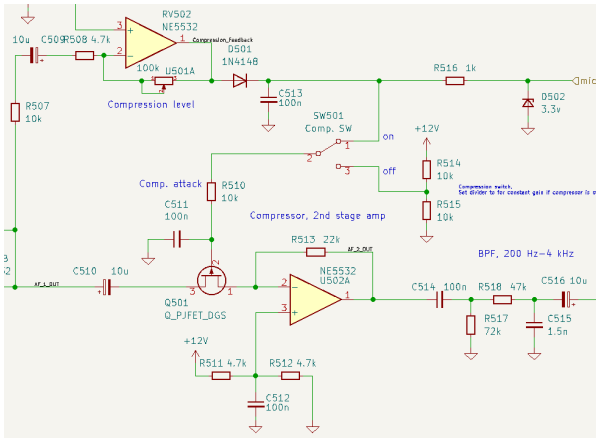


Figure 2.3: Schematic of audio compressor

Level of compression can also be controlled by the potentiometer. Furthermore the attack of compressor can be set by changing values of RC network that smooths the DC voltage. Output from a compressor passes then through a LC band pass filter. In order not to load the filter with low impedance and thus changing its characteristics a buffer impedance op amp is used. This does not cost anything because two NE5532 have to be used for this circuit anyway and one IC already contains two op amps giving four in total. In theory this circuit can work with just two op amps but then DC control voltage is less independent of the gain and setting proper levels might be difficult.

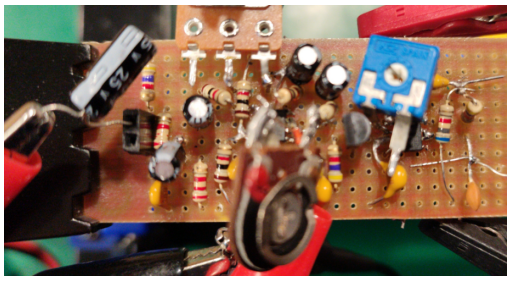

Figure 2.4: Prototype of audio stages

Prototype of the circuit was tested and a compression knee was plotted. Gain potentiometer was set to the middle position (12 o'clock). The input amplitude of 1 KHz sine wave was increased. The gain potentiometer was set to middle, maximum and to a minimum (5.7 V was set as a control voltage with no feedback loop to disable compression).

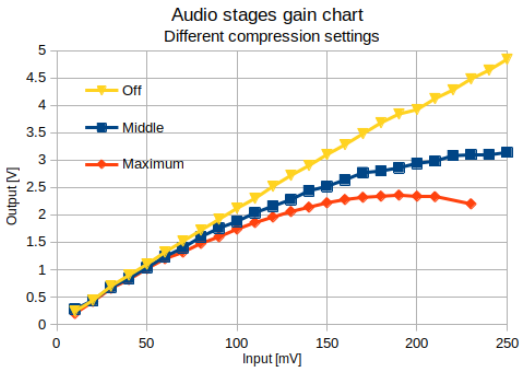


Figure 2.5: Compressor characteristics measured from a prototype

In the fig. 2.5 it can be seen that the compression circuit is indeed working. Test with disabled compression has shown that the amplifier works with linear voltage gain. With a medium setting compression knee is soft and less compression is applied in comparison to a maximum compression. Threshold of compression for given setting of microphone gain is about 100 mV which is realistic value for a preamplified microphone. User should first set the compression to minimum and then adjust the gain of microphone, then compression level can be adjusted since control voltage is derived from the first microphone stage. In the next test a response of the circuit in frequency domain was characterized.

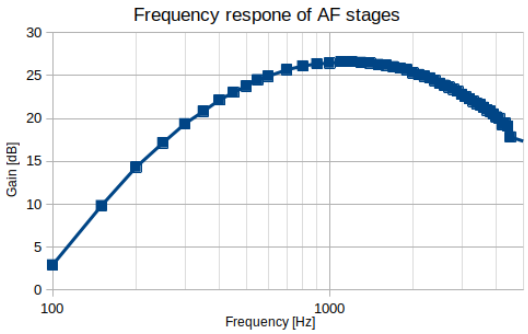


Figure 2.6: AF response characteristics measured from a prototype

It can be seen in fig. 2.6 that the response is not flat in the pass band as it ideally should be. The -3dB bandwidth is 2.6 Khz (450 Hz to 3 KHz). Especially the lower cut off frequency could be decreased but for now it will be left in this form for further tests.

## 2.2 Local oscillator

This stage provides sinusoidal waveform for a double balanced mixer. Signal should be clean from distortion and stable in frequency. Because local oscillator needs to give just one frequency a crystal resonator will be used.

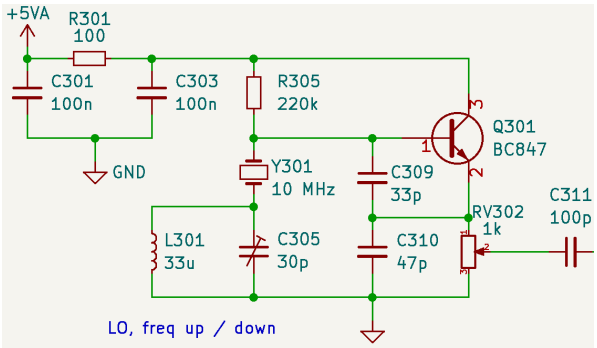


Figure 2.7: Schematic of the LO

Colpitts topology was chosen because it can operate with stable high frequency in a wide temperature range. Recommendations for the values were taken from the Crystal Oscillator Circuits by Robert J. Matthys[17]. Signal from oscillator was sourced from emitter by the use of potentiometer in order to control input level to the balanced mixer.
Note that L301 and C305 are added in series with the crystal in order to precisely tune the LO frequency. This is so that the carrier can be put 300 Hz apart from the -3 dB point of the SSB filter. Components with low temperature drift should be used in this place.

Frequency of the local oscillator was chosen as 10 MHz. This is because crystals with that resonant point are easy to obtain and also because it is a value in between two popular ham bands: 40 m (7 MHz) and 20 m (14 MHz) giving enough room for filtering out unwanted signals. Choice of lower frequency for stage is often dictated by the fact that low frequency is easier to process and noise of the components is lower, however the end result is 14 MHz which by nowadays standards is not that high and high frequency effects don't play significant role in choosing process of local oscillator.
Pilot crystal for the LO can be taken from a batch of crystals that were used to create an SSB filter for close frequency match.

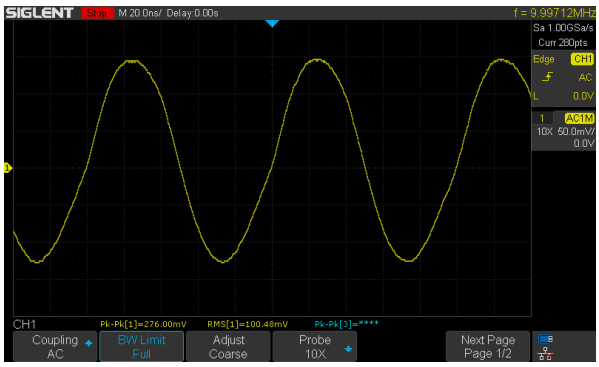


Figure 2.8: Waveform of LO output

It can be seen that the waveform has some distortions however this is not crucial for the operation because the signal will be passed by the filter anyway. For further inspection in frequency domain a signal analyzer was used. Note that the spectrum analyzer has termination of 50Ω so the measurement does not portray amplitude levels during normal operation. Focus of this test was just to observe the harmonics.

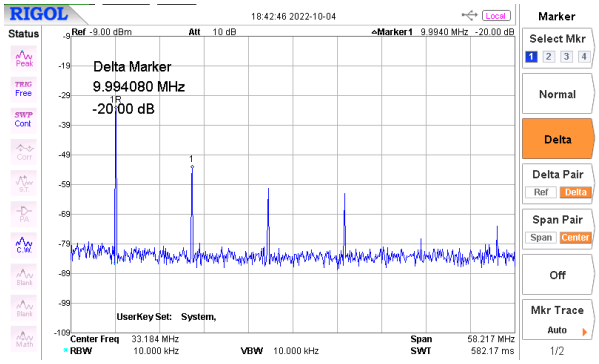


Figure 2.9: Spectrum of the LO

It can be seen that distortions in time domain from fig. 2.8 are visible as harmonics in fig. 2.9. First harmonic is 20 dB below the fundamental signal which is an acceptable level for this purpose since output from a balanced mixer will be passed through a steep filter.

## 2.3 DSB generator

### 2.3.1 Double balanced mixer

A mixer is a three-port circuit with two input signals and one output occurring at frequency that is the sum and/or difference of the two input frequencies[6].
Standard mixer outputs sum and differences of two signals, so if we use the LO and AF signals from previous stages the result would be an AM signal with significant carrier. In order to reduce LO signal from appearing at the output a balanced mixer is used. Such circuits are symmetrical, providing a balance of inputs results in no net current in two differential pairs resulting in suppression of LO at the output.
Such a solution is implemented in NE602.

### 2.3.2 NE602

This IC is a double balanced mixer using Gilbert transconductance cell[11].

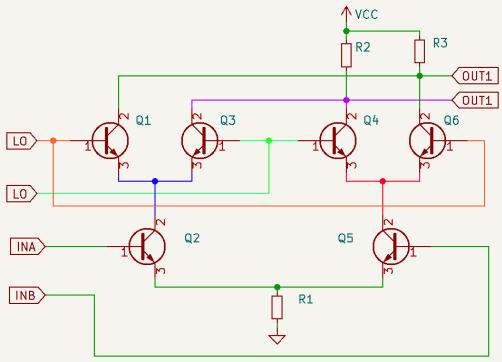


Figure 2.10: Schematic of a Gilbert cell

Gilbert cell consists of two symmetric differential pairs (Q1, Q3 and Q4, Q6) and a pair of transistors that control the current flowing though differential pairs (Q2 and Q5, this can also be seen as a third differential pair). The principle is that if the bottom pair is in balance the currents $I_{CQ2}$ and $I_{CQ5}$ are the same and thus there is no potential created by upper pairs across the load resistors R2 and R3. This reduction in local oscillator output creates a double sideband signal, basically an AM with suppressed carrier. One can expect a 30 dB of carrier suppression with this circuit[6].

NE602 also has an internal oscillator that operates up to 200 MHz with an external LC tank, external input can be provided for operation up to 500 MHz. Typical third order intercept is -13 dBm and conversion gain of about 17dB[19]. We can be sure that this IC can operate on desired frequency, it has not the best dynamic range but it is an active mixer meaning it has positive conversion gain so further amplification won't be necessary and smaller footprint will be possible.

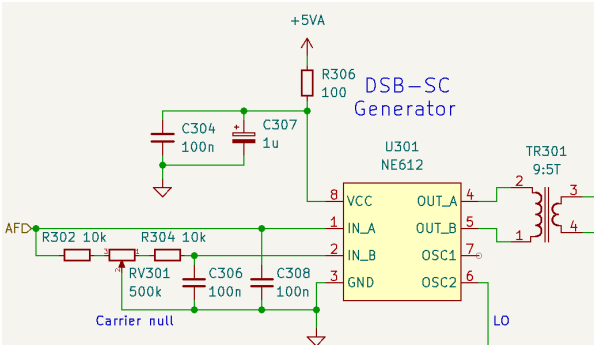


Figure 2.11: Schematic of NE602 as a balanced mixer

NE602 draws less than 2.5 mA current at 5 V and 25 C°, 100Ω resistor with a 100n and $1\mu F$ capacitor provide decoupling for the mixer. Because of low current no significant drop occurs on this resistor (only 0.25 V leaving 0.5 V of headroom).

NE602 has internal bias network so external voltage source is not necessary, network of external resistors (R302, R304) and potentiometer RV301 are used to balance the mixer.

Local oscillator input is fed to the internal buffer through a pin 6 utilizing a single ended drive option.
Output however uses differential configuration for harmonic suppression. This option is also convenient because output transformer will be used to match 1.5 k output impedance of the mixer to the following SSB filter.

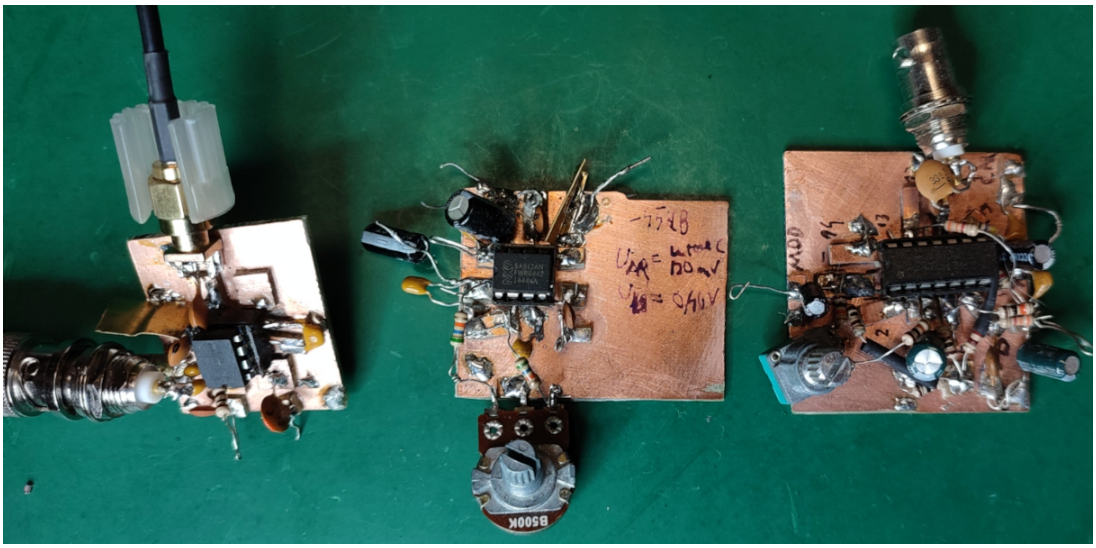

Figure 2.12: Evaluation circuits on copper boards, from left: NE602 mixer, NE602 double balanced mixer, MC1496 double balanced mixer

Circuit from figure 2.11 was first assembled on a copper board using a DIP-8 package. This prototype was then evaluated using external DDS generator and spectrum analyzer for best level of input of AF and LO optimizing carrier suppression and spurious free dynamic range (SFDR).

With AF input of 1 KHz sinusoidal signal with amplitude of 120 $mV_{pp}$ and 10 MHz carrier of 0.46 $V_{pp}$ a signal was observed. Output was terminated to a 50 Ω load.

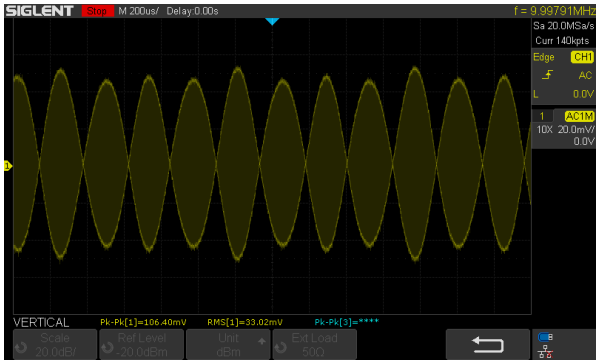


Figure 2.13: Output from balanced NE602

As it is shown in fig. 2.13 the waveform looks like AM with very high depth of modulation. We should investigate the frequency domain in order to determine the carrier suppression.

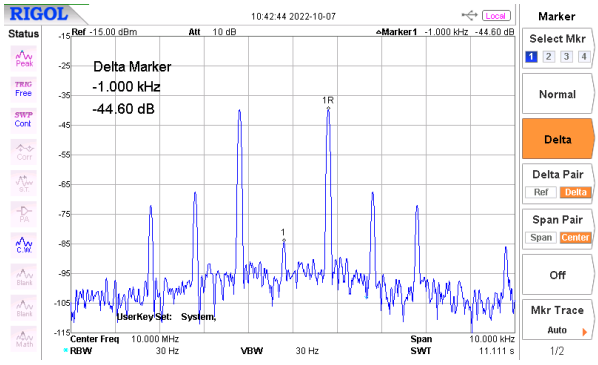


Figure 2.14: Spectrum of NE602 output

Output is indeed a double sideband. The sidebands are as expected 1 KHz apart from the carrier. The carrier itself is attenuated by 44 dB which is a very good result. Spurious signals are harmonics of the 1 KHz modulating signal, giving SFDR of almost 30 dB which is sufficient for our application since the transmitter won't be operating with high enough power for those spurs to affect audio quality at the receiving end.

### 2.3.3 MC1496

Another IC that uses Gilbert cell and can be used for DSB generation is MC1496p. This part is in a larger 14 pin package and requires a lot more external components although the basis of operation is similar. External load resistors and bias might

be useful when designing circuit with particular requirements (NE602 uses internal 1.5k resistors for differential pairs collectors). MC1496 can be operated from a higher voltage of 12 V which is popular in amateur radio but it also draws more current of up to 10 mA[18]. Gain can also be controlled with a resistor. One significant advantage of MC1496 is that it's data sheet is much more complete, manufacturer provides a claim of -50 dB carrier suppression at 10 MHz. Graphs of carrier suppression against carrier input levels and carrier feed through are also provided alongside example circuits. One of those circuits for a balanced modulator supplied from a single rail was chosen for evaluation of the IC (see fig. 2.15).

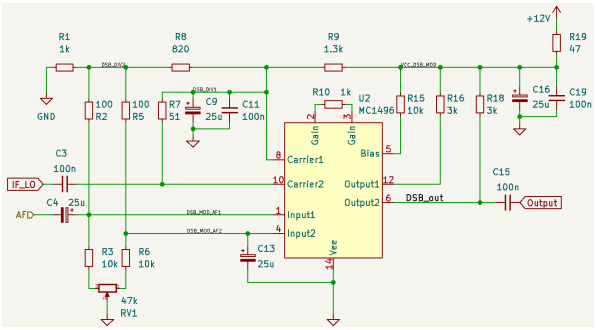


Figure 2.15: Schematic of balanced mixer with MC1496p

Again the circuit was assembled on the copper board and evaluated like NE602 (see fig. 2.12). This time only the spectrum domain was observed. Carrier was a 10 MHz sine wave but amplitude of 120 $mV_{pp}$ and the modulating signal was 1 KHz signal with an amplitude of 350 mV.

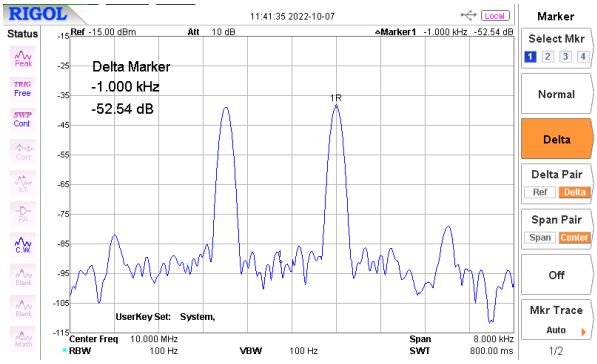


Figure 2.16: Spectrum from MC1496p

As it is shown in fig. 2.16 the carrier attenuation is order of magnitude better giving 52 dB of attenuation. The SFDR is also better being 40 dB.
Amplitude of output for both mixers seems to be very similar. Overall in this case MC1496 seems to give more desired signal. However it has a larger footprint especially when all the external parts are considered. Since the aim is to build a working transmitter and knowing that it is easier to obtain in SMD package, NE602 fulfills our requirements. Role of a double balanced mixer in this project will take the NE602.

## 2.4 SSB filter

Having a double sideband with suppressed carrier in order to obtain SSB we should use a very selective filter (being able to reject relatively closely adjacent signals). According to ITU recommendations the slope of the transmitter's response should be at least 35 dB/KHz[8]. Since a typical bandwidth used for SSB on amateur band ranges from 2.4 KHz to 2.7 KHz a -3 dB bandwidth of 2.7 KHz will be taken as a goal for filter construction. Next consideration is a ripple in the passband, here 1 dB will be assumed as acceptable.

### 2.4.1 Crystal parameters

In order to achieve such a steep response of a filter a very high Q tuned circuit has to be used. Normal construction of such a LC tank would be impractical however a very common crystal quartz oscillators are in fact a very high Q LC tanks and can be treated as a connection of relatively large inductor and very small capacitor in series. Therefore such crystals are seen as a very high Q LC circuit. Equivalent model of a crystal resonator is shown in a fig. 2.17.

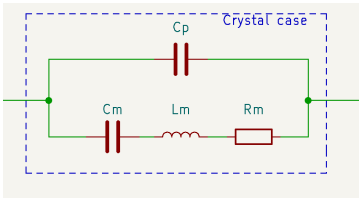


Figure 2.17: Model of a crystal

$C_p$ is a parasitic capacitance of a housing. Motional inductance $L_m$ and motional capacitance $C_m$ are primary factors determining the crystal's resonant frequency. Looking at the figure 2.17 it can be deduced that maximizing motional inductance and minimizing series resistance and capacitance will cause the circuit's Q to rise. Higher Q translates to a more narrow bandwidth of a resonance. In order to observe the response of a crystal resonator a spectrum analyzer was used with a simple fixture that allowed for direct connection of one crystal lead to a tracking generator and a second lead to instrument's input. 10 MHz crystal was investigated.

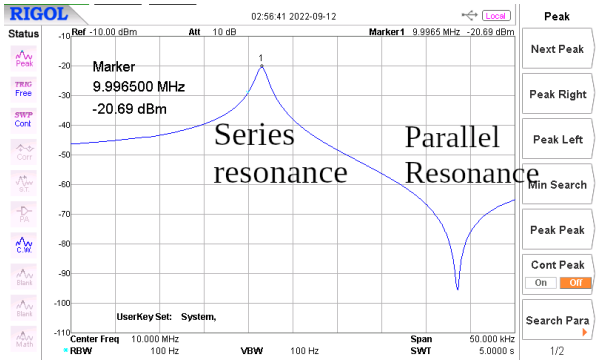


Figure 2.18: Measurement of a crystal

In the figure 2.18 sweep of 50 KHz was presented. One can see that crystal does in fact create a high Q circuit. The series resonance is a point where impedance at a given frequency is very low. Knowing that the output of tracking generator was set to -20 dBm insertion loss was measured to be to 0.69 dB. This loss is mainly caused by the mechanical resistance ($R_m$ in fig. 2.17) which also decreases the Q.

### 2.4.2 Crystal ladder filter

Overall the shape of series resonance curve can be used to our advantage. Normally the bandwidth of a single crystal is not enough to create a sufficient wide filter nor is it flat. That is why multiple crystals in series are used with capacitors that shift their center frequency of series resonance creating a circuit with even sharper characteristics and desired passband[6].

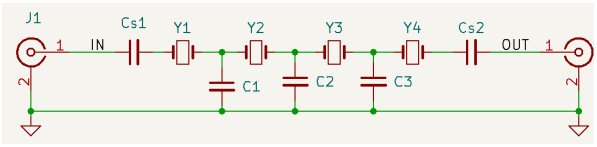


Figure 2.19: Schematic of a 4 crystal ladder filter

Steepness of the filter can be increased by cascading more crystals. Values of the series capacitors (Cs1 and Cs2) are the same and are used in the circuit for tuning. The C1, C2, C3 are coupling capacitors or shunt capacitors. Values of those capacitors can be calculated knowing the motional parameters of crystals chosen for the filter[23].

Figure 2.20: Crystals divided into smaller batches based on histogram

All crystals used for the filter should have as close resonance point as possible. Parameters like the motional capacitance or inductance are usually not given by the manufacturer. That is why a pack of 50 10 MHz crystals was bought. All 50 crystals were first measured for oscillating frequency in a simple Colpitts oscillator and frequencies were noted from an oscilloscope. Histogram of examined batch was created in order to find suitable crystals for ladder

filter and for matching pilot LO crystal.

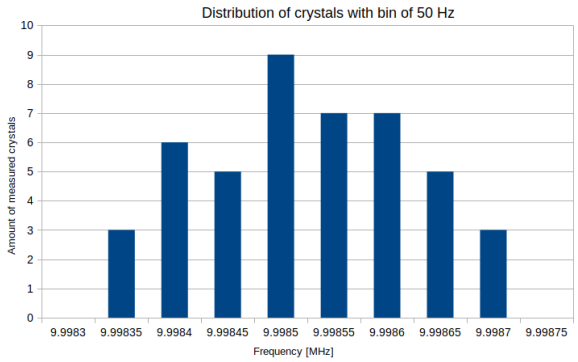


Figure 2.21: Histogram of examined batch

From a histogram with more narrow bins two sets of 4 crystals were selected. Each set had resonances within 10 Hz. For those 8 crystals series of more detailed measurements was conducted. Determination of motional parameters would require specialized apparatus that is not easily available, that is why a two indirect methods will be presented.

### G3UUR method

This method is popular among amateur radio operators. It uses Colpitts oscillator for a crystal with one lead of the crystal either being grounded or being connected in series with a known capacitor usually 33 pF or 47 pF. The oscillator is connected to a frequency counter or to an oscilloscope and two frequencies are noted: one with shorted lead and one with capacitor in series[25]. Knowing shift in oscillation ($\Delta f$), introduced series capacitance $C_s$ and parasitic holder capacitance $C_p$ the motional parameters can be determined using equations:

$$C_m = 2(C_s + C_p)\frac{\Delta f}{f} \tag{2.1}$$

$$L_m = \frac{1}{2\pi f}C_m \tag{2.2}$$

For example one crystal was measured to create a sinusoidal signal of 9.99863 MHz with grounded lead and 9.9998282 with 33 pF capacitor connected in series, so the series connection increased frequency by 1.19 KHz. From that value of $C_m$ was calculated to be 11.56 fF and $L_m$ was calculated as 21.91 mH. It can be seen that the value of capacitance is indeed very small while the inductance presented by the circuit is relatively high.

Next we should determine the capacitance that is present between the leads. For that an LCR meter can be used with a crystal connected directly to a meter. Measurement should be made at a low frequency and the expected value is between 3 to 6 pF[24]. For investigated crystal the $C_p$ was determined to be 3.6 pF.

G3UUR method does not provide a method for determination of mechanical resistance and thus we don't know the Q of a crystal. One can use a 50Ω signal generator with high resolution and an RF detector like input terminated oscilloscope or an millivoltmeter with RF probe in order to determine a -3 dB points of the crystal series resonance. Such analysis of methods was presented by Nick Kennedy WA5BDU in his presentation "Crystal characterization and crystal filter design" [13] however in next method a signal analyzer will be used for that which should provide better resolution and accuracy of measurement however it is less accessible method for some experimenters.

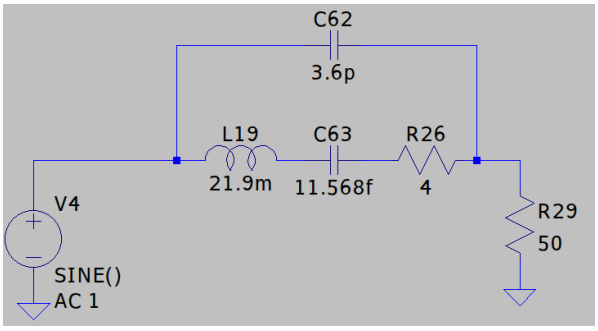


Figure 2.22: Schematic of modeled crystal and spice test setup

Assuming for now that the value of mechanical resistance is 4 Ω it is possible to model the crystal in spice software.

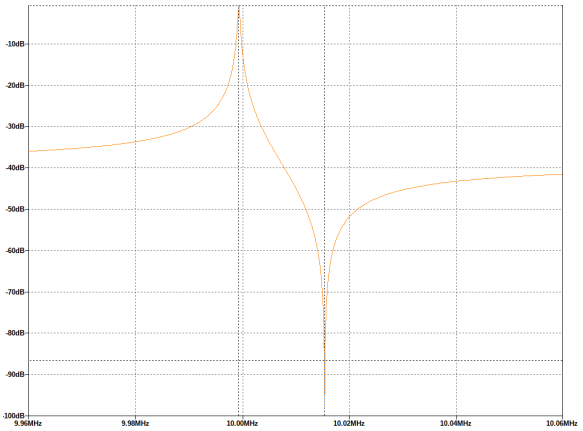


Figure 2.23: Simulation of modeled crystal

Looking at the figure 2.23 it can be seen that it does look like characteristics from fig. 2.18 where real crystal from the same batch was tested with spectrum analyzer.

In order to determine if the method is indeed precise a spectrum analyzer was used to determine the series and parallel resonance of the investigated crystal. Results alongside accuracy of G3UUR simulated crystal were noted in a table 2.1. Presented method works and error is very small, for our purposes is negligible.

| **Simulated** | | **Real crystal** | | $\delta$ | |
|---|---|---|---|---|---|
| Fs [MHz] | Fp [MHz] | Fs [MHz] | Fp [MHz] | Fs [%] | Fp [%] |
| 9.9993 | 10.0153 | 9.996835 | 10.016404 | 0.025 | -0.011 |

Table 2.1: Characteristic of Spice simulated crystal from G3UUR method for a real crystal tested using spectrum analyzer

### Series parallel method

As it was mentioned in the previous subsection the G3UUR method does not provide a mechanical resistance of the crystal and thus we don't know the Q. This does not prevent construction of a filter however knowing Q assures choice of crystals with lowest insertion loss and best steepness.

Another amateur radio operator, Jack R. Smith K8ZOA has compared G3UUR and other methods against professional standard in his paper[22]. This paper presents G3UUR method, phase shift method, -3 dB bandwidth method, series and parallel resonance method for a Saunders & Associates Reference Crystal and compares these methods to a measurement made using automatic characterization function of HP87510A.
Series and parallel method is based on measurement of two characteristic resonance points of a crystal. For that a spectrum analyzer is the best tool. Whole batch of crystals was once again measured like in fig. 2.18. Insertion loss, series and parallel resonance points were noted for each crystal in a spreadsheet. The motional parameters in this method are calculated using equations:

$$C_m = \left(\frac{f_p}{f_s} - 1\right) \cdot 2C_p$$

$$L_m = \frac{1}{(2\pi f_s)^2 \cdot C_m}$$

With this method an insertion loss ($-S21$) can be measured as the difference between peak of the series resonance magnitude and tracking generator reference level. Knowing the S21 loss and input power a mechanical resistance ($R_m$) can be calculated as:

$$R_m = 2 \cdot R_L \left(10^{\frac{-S21}{P_{in}}} - 1\right) \tag{2.3}$$

Knowing that $R_L$ is a load impedance, in our case 50 Ω of spectrum analyzer the resistance of the investigated crystal was calculated to be 9.65 Ω so much higher than estimated but still in correct order of magnitude. Bandwidth can be defined as a ratio of a central frequency over Q. Higher the Q more narrow the bandwidth is, for a given crystal Q was calculated to be 4.92E+19.

| Measured | | | | | | Calculated G3UUR | | Series and parallel | | | |
|---|---|---|---|---|---|---|---|---|---|---|---|
| nr | FG[MHz] | FCs[MHz] | s21[dB] | Fs[MHz] | Fp[MHz] | Cm[fF] | Lm[mH] | Cm[fF] | Lm[mH] | Q | Rm |
| 1 | 9.99863 | 9.99982 | -0.8 | 9.996835 | 10.016404 | 11.568 | 21.910 | 14.098 | 17.997 | 4.92E+019 | 9.65 |
| 2 | 9.99863 | 9.99978 | -1.9 | 9.996797 | 10.016133 | 11.180 | 22.673 | 13.930 | 18.214 | 4.80E+019 | 24.45 |
| 3 | 9.99863 | 9.9999 | -0.5 | 9.996785 | 10.016133 | 12.346 | 20.530 | 13.939 | 18.203 | 4.80E+019 | 5.93 |
| 4 | 9.99862 | 9.99988 | -0.8 | 9.996741 | 10.01725 | 12.249 | 20.693 | 14.775 | 17.172 | 5.40E+019 | 9.65 |

Table 2.2: Measurements for two methods of evaluating the motional parameters of crystal resonator with results. Colors correspond to method used and data gathered for that method.

**Conclusion on determination of motional parameters**

The amateur radio community in necessity of crystal characterization has developed and compared quite a few methods that provide reliable results.
In fact, a paper by Jack R. Smith (K8ZOA) shows that G3UUR method has error lower than 5% in comparison to a professional equipment[22] which seems to confirm measurements conducted here. All measurements and calculations for crystals that will be used in created SSB filter are presented in table 2.2.

### 2.4.3 Filter components calculation and simulation

Knowing the parameters of used crystals and desired parameters model the entire filter can be simulated. A Dishal program created by Horst Steder (DJ6EV) will be used for that.
Input parameters will be set as following:

- Bandwidth 2.7 KHz
- Series frequency 9999.82 KHz
- $L_m$: 21.45 mH
- $C_p$: 3.6 pF
- Ripple in passband: 1 dB
- Type of filter: Chebychev
- Number of crystals: 4

The Chebychev filter was chosen for this application because of its steepness. This filter has some ripple and ringing which can cause the audio to be distorted, also a delay makes it unsuitable for digital modes[13]. However in order to meet the ITU recommendations it is good compromise between quality of the audio and steepness.

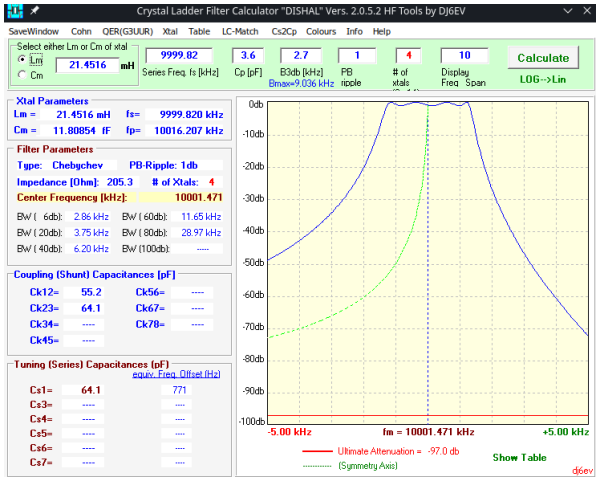


Figure 2.24: Dishal filter calculator

Dishal calculates not only the necessary capacitors but also determines the impedance of the filter. Unmatched crystal filter will be effectively seen as if it had much higher ripple.

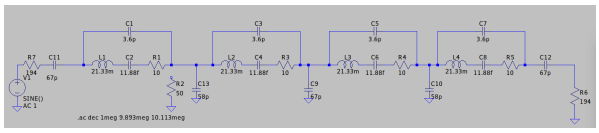

Figure 2.25: Spice simulation of filter

Knowing the values of capacitance, spice simulation of a filter from fig. 2.27 was ran. End of the filter was terminated with a resistor in order to present it with matched

impedance. Therefore the insertion loss was very high but selectivity and shape of the filter remained correct.

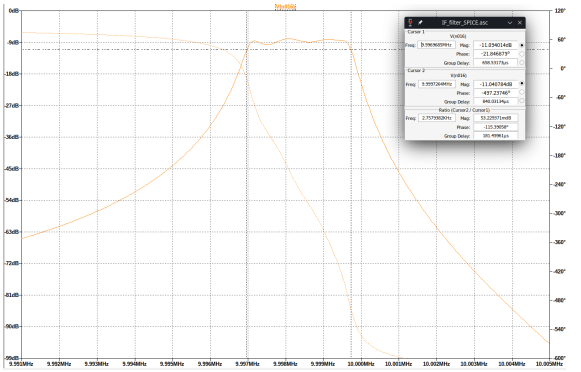

Figure 2.26: Spice simulation of a ladder filter with 4 crystals

It can be seen in the figure 2.26 the filter has -3 dB bandwidth of 2.75 KHz so almost exactly to that what was desired. The passband ripple is 0.86 dB so below allowed 1 dB.

When it comes to steepness it can be seen that this filter has not symmetrical characteristics. The low side is less steep due to parasitic capacitance between the leads and case of the crystal ($C_p$)[13]. Wes Hayward in EMRFD[6] has described possible method of compensation for this effect. Effect itself is especially problematic when it is necessary to reject the lower sideband. This leads to a poor low sideband attenuation favoring the upper sideband rejection with this kind of filter. That is why a second mixer will use up conversion method where input frequency to a mixer is higher than the desired output. This requires much higher frequency of the VFO but it allows filter to create better image of LSB signal that is then symmetrically flipped creating eventually USB signal.

At this point values for 6 and 8 crystal filters were also calculated and those filters were simulated for a comparison.

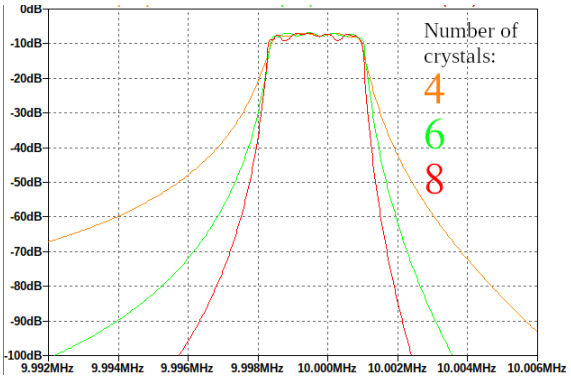


Figure 2.27: Comparison of 4, 6, 8 crystal filters in LTspice

As it was shown, with more crystals the filter becomes steeper. In simulation the right slope of the filter was compared. From a -3 dB cutoff point for each filter a db/KHz was determined. The same was repeated for a lower side of the filter.

In the table 2.3 the amount of 6 crystals seems to be sufficient for meeting the ITU recommendations, because of a small batch of crystals in this project a 4 crystal filter will be built. It is also worth noting that for a 4 crystal filter the the ratio of upper side to lower side steepness is 39% while for the 8 crystal filter this ratio decreases to 28%.

| **Number of crystals** | **Slope [dB/Khz]** | |
|---|---|---|
| | **Low** | **High** |
| 4 | 23 | 32 |
| 6 | 40 | 52 |
| 8 | 57 | 73 |

Table 2.3: Steepness of upper and lower slope of ladder filter with n crystals (according to a simulation based on measured motional parameters of generic 10 MHz crystal)

### 2.4.4 Real filter construction and impedance matching

PCB for 4 and 8 crystal filter was designed as a module that can be mounted on a RF board of transmitter. The filter was assembled with the use of NPO capacitors for low drift due to temperature. Sides of the PCB were cut in order to use larger vias inside tin as an improvised castellated edges.

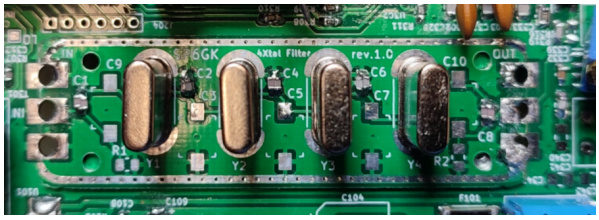

Figure 2.28: Assembled crystal filter

In order to test the filter with spectrum analyzer two potentiometers were connected on the input and output in series with coaxial cables to the spectrum analyzer. The tracking generator was turned on and potentiometers were tuned for the lowest ripple of the filter. This method ensures the impedance match of the test setup however it adds a great attenuation (almost 40 dB) but this factor is not important as long as the majority of the signal is above the noise floor of the instrument.

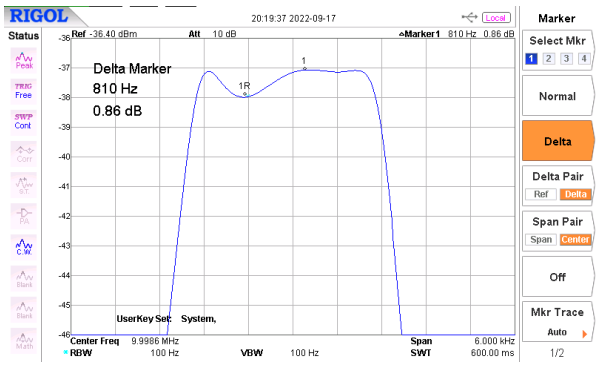


Figure 2.29: Measurement of passband

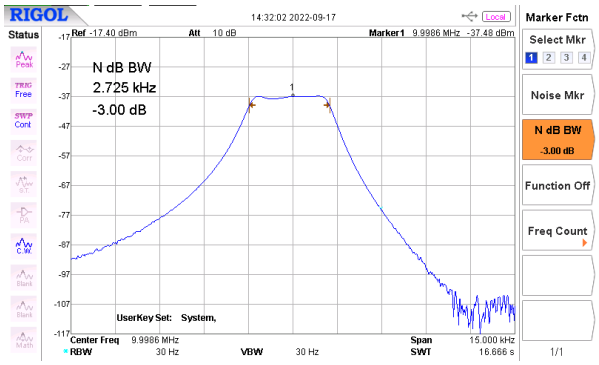


Figure 2.30: Wider look at the created filter

Looking at the left side of the filter it can be seen that it is in fact less steep. Just before the cutoff the slope is 26 dB/KHz. On the upper side the slope is steeper and slope is 37 dB/KHz. So in fact the result of steepness is a bit better than in simulation (table 2.3). This is close to ITU recommendations but not quite enough. It is enough however for home experiment.

**Impedance matching of the filter**

Tuning the potentiometers connected in series with the filter were disconnected and measured with ohmmeter. Value was determined to be 250 Ω This impedance is higher than the one calculated by Dishal calculator.

We know that mixer's output impedance is 1.5k. Input of mixer is also 1.5k so we need to transform the impedance otherwise reflections will occur and passband will have significant ripples.
The total impedance that needs to be matched is the sum of spectrum analyzer termination and the measured value from potentiometer:

$$Z_{filter} = 250\Omega + 50\Omega \tag{2.4}$$

The ratio of impedance and transformer ratio are given as:

$$Z_{ratio} = \frac{Z_{filter}}{Z_{mixer}} = 0.16$$

$$T_{ratio} = \sqrt{\frac{300}{1500}} = 0.447$$

We have to get number of turns as close to an integer as possible:

$$2 \cdot 0.447 = 0.894$$
$$3 \cdot 0.447 = 1.341$$
$$\vdots$$
$$9 \cdot 0.447 = 4.917 \approx 5$$

Ratio of turns 9:5 is a close solution. This means 9 turns on the primary side (side of mixer) and 5 turns on secondary side (input to the filter). This configuration is known as balanced wide band transformer.
Different core materials can be used for such a circuit. For good coupling and small size a torioidal transformer core will be used, FT50-43 is a 43 ferrite type core typical for such applications. Transformer was wound with an enameled wire of 0.37 mm diameter. For a test of impedance matching a manual sweep of audio frequency was done using a signal generator at the input of the DSB mixer and output from second transformer was measured point by point. Output was noted in spreadsheet and plot of response was created.
Local oscillator was at this point tuned to frequency 350 Hz below the -3 dB of lower side cutoff of the filter. Frequency was marked on horizontal axis with carrier being denoted as a zero and step of 100 Hz was taken. The vertical scale is logarithmic in dB.

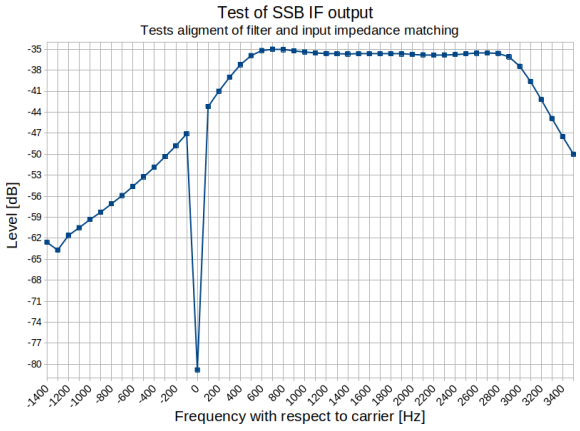


Figure 2.31: Response at the filter output of assembled circuit

In the figure 2.34 it can be seen that the -3 dB bandwidth is in fact 2.7 KHz as intended. What is more important the passband is relatively flat and therefore we have properly matched the impedance between the stages. Attenuation of carrier is also visible since there is practically no signal. Carrier is also approximately 350 Hz away from the passband giving modulator the audio bandwidth of 350 Hz to 3.05 KHz which in deed can be used for narrow voice transmission. The figure 2.34 is also important because it shows the problem with shape of the filter, the lower sideband starts 350 Hz below the sideband and at this level there is only 12 dB of attenuation. This is not satisfactory solution for upper sideband modulation, rejection of sideband should exceed 30 dB. Proposal for solution for this problem is either compensation of $C_p$ that is affecting shape of crystal characteristics or change of sideband and then flipping it symmetrically by up conversion with higher frequency of VFO in next stage.
Next a spectrum analyzer was used to examine created SSB USB signal with single tone input.

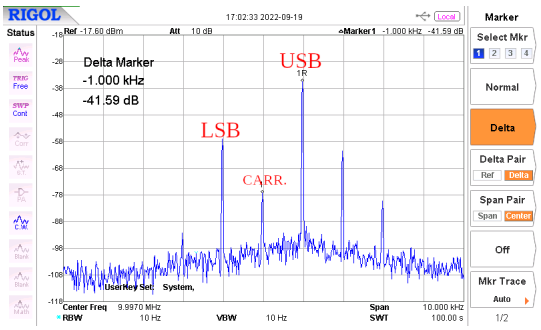


Figure 2.32: SSB output for 1 KHz input signal

Observing response for the single tone 1 KHz sinusoidal signal it can be seen that the carrier attenuation is more than 40 dB which is very good. However the sideband is suppressed by only 20 dB. This situation is worse for 300 Hz where suppression is only 11 dB. This is due to less steep slope of the lower side of the filter, later on a correction can be applied by change of sidebands and proper tuning of VFO. The spurs on the right side are the result of non linearity of the mixers and are harmonics of mod-

ulating signal, they affect quality of audio signal but for voice transmission their level is acceptable.

## 2.5 VFO

VFO stands for variable frequency oscillator. Since processing of SSB signal is carried at single constant frequency (intermediate frequency or IF) we need an oscillator and a mixer that will shift the ready signal to a desired transmit frequency. The oscillator should allow the operator for easy tuning in the range of entire band. This oscillator should also be stable in frequency.
Back in the day a varicap diode with an LC circuit or just an LC circuit with variable air capacitor were popular solutions however both suffered from drift problems. Nowadays digital direct synthesis (DDS) presents cheap wide frequency and more importantly stable source of oscillations.

### 2.5.1 Theory of DDS

Goal is to create a sine wave that can be changed in frequency by the user.
This is not easy with digital circuit because $a(t) = sin(\omega t)$ is a nonlinear functions in terms of magnitude and therefore it is difficult to generate it. Sinus waveform is however linear in terms of phase so it is possible to relate the necessary information to an angular rate $\omega$[2] having a reference clock period $\Delta t$.

$$\Delta phase = \omega \Delta t \tag{2.5}$$

$$\omega = \frac{\Delta phase}{\Delta t} = \frac{2\pi}{f} \tag{2.6}$$

$$f = \Delta phase \cdot \frac{f_{mclk}}{2\pi} \tag{2.7}$$

DDS has a numerically controlled oscillator that uses information from registers and reads phase information from ROM. DAC is then used to create analog output.
In the case of discussed design a DDS that can generate at least 24.35 MHz is necessary. Because of Nyquist-Shanon law the clock of DDS needs to work with twice that frequency. Suitable integrated DDS is available from Analog Devices. AD9834 is a low power fully integrated DDS IC, it has 10 bit DAC and master clock can operate up to 75 MHz. Because such a generator was not present at the market at that time a closest crystal based generator will be used - 66 MHz. This leaves maximum frequency at 33 MHz. There is some room for over sampling since DACs usually have lower noise density (NSD) at lower frequency of operation. Choosing a crystal generator that is stable with temperature benefits this solution. Phase noise or jitter is also important on the DAC performance.

### 2.5.2 Implementation of DDS

Implementation of AD9834 requires some external components, mainly capacitors for decoupling. Those should be placed closely to the IC, especially those for decoupling of an internal 2.5 V reference for the DAC. Analog line for the AD9834 is filtered by ferrite bead and 100 nF capacitor. In order to prevent series resonance a 1 uF capacitor was added, because of its larger ESR the series oscillation is damped. For better EMI a 100 Ω resistors are added to a SPI ports, communication does not have to be very fast. This simple solution should limit fast transients and ringing on the digital traces.

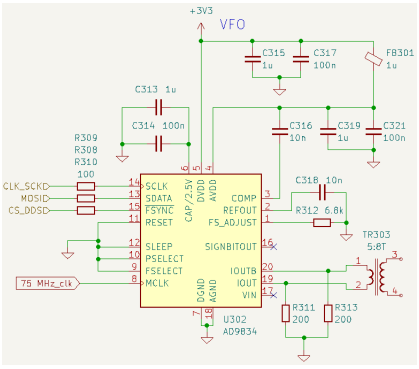


Figure 2.33: Schematic of AD9834 implementation in transmitter

Since DAC produces approximation of analog signal with only 10 bits of resolution and not that high oversampling some noise is bound to appear in the output signal. Therefore output of the DDS was tested. Program for STM32F411 was written to produce 14 MHz with AD9834, output was observed using an oscilloscope and spectrum analyzer.

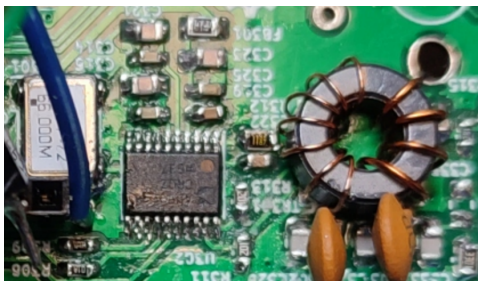

Figure 2.34: AD9834 with matching transformer and LPF on the PCB

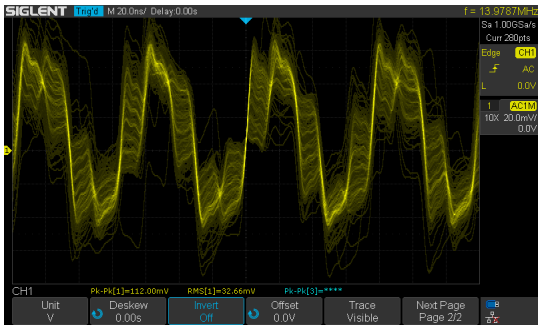


Figure 2.35: Output of AD9834 with no filter for 14 MHz sine in time domain

Looking at the figures 2.43a and 2.43b it can be seen that before passing this signal further some low pass filter should be applied. This filter will reconstruct fundamental to be a cleaner sine wave.
Design of this low pass filter follows the procedure presented in EMRFD book[6]. Because the filter will have to have some defined impedance and one of the design goal is to keep the output level across the band constant we should match the impedance of DDS to the filter and mixer. Keeping constant level of the VFO is important because it will be one of the factors that affect RF output level across the band, also if a new goal was to redesign transmitter to work on another band (or add it) it saves a lot of time to have a wide and flat response of the VFO. We know that the impedance output of the AD9834 (integrated DDS chip) is 200 Ω because of the terminating resistors R311 and R313. Using the procedure from section 2.4.4 a matching wide band transformer was calculated with ratio 5 primary turns to 8 secondary turns.
At this stage we have DDS output with impedance of 1.5k and mixer input also with 1.5k impedance. We can therefore calculate a LPF with 1.5k impedance for a match.
Because of the low ripple (flat response in passband) requirement a filter described Butterworth polynomial will be chosen. This type prioritizes a flat passband by the cost of less steep of roll off.
Design of a filter starts with normalized values $g(n)$ of components that describe filter for 1 Ω termination and cut off frequency of $\frac{1}{2\pi}$ Hz. These values are later scaled[6]. Here a 4th order filter will be designed, for that we have two inductors and two capacitors so two parts of the circuit can be imagined each being an L topology of low pass LC circuit. From a table of normalized: $g(n)$ for N=2 Butterworth is 1.414 and 1.414. Taking n as a part of the circuit (not the order but rather section of physical circuit in this case n is 1 or 2), inductance and capacitance necessary can be calculated:

$$L(n) = \frac{g(n) \cdot R_0}{2\pi f} \tag{2.8}$$

$$C(n) = \frac{g(n)}{R_0 \cdot 2\pi f} \tag{2.9}$$

Where $R_0$ is an impedance termination (this is a doubly-terminated circuit) and $f$ is an edge of the pass band (not the cut off). Since the 4th order filter uses the same $g(n)$ values for both parts of the circuit the components are easier to source. With given values inductors were calculated as 12 uH and capacitors as 5.3pF. Since these are not E24 series numbers, the closest values will be used in simulation. Once again the circuit was recreated in LTspice.

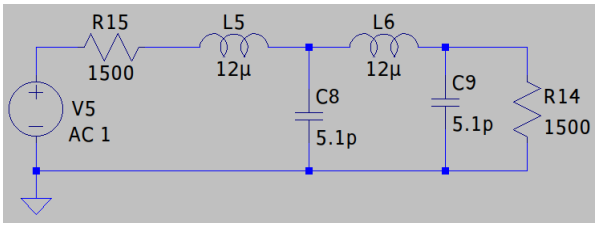


Figure 2.36: Schematic of designed LPF

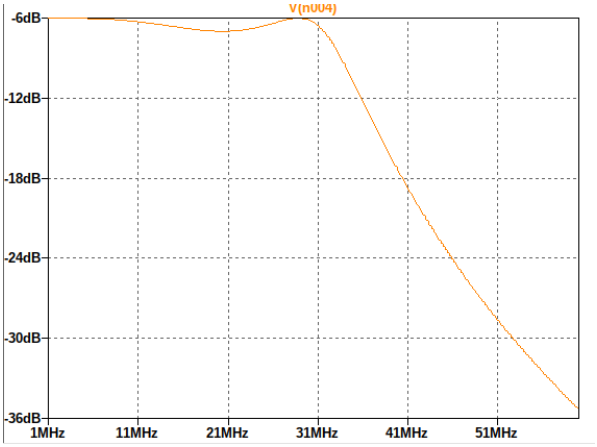


Figure 2.37: Simulation of the DDS filter

Using cursors to read the crucial characteristic of the filter in figure ?? it was determined that the ripple is only 0.92 dB. Peak at the upper side of the passband is at 29 MHz, this is probably due to the choice of 5.1 pF E24 capacitors instead of 5.3 pF as calculated. The -3 dB cut off is at 33 MHz, attenuation at 58 MHz (octave from 29 MHz) is 28 dB.

Filter was then assembled on the PCB and VFO was set to 24 MHz since that is the typical frequency that will be used for transmit mixer. Looking at the figure 2.38d and 2.38c it can be seen that the designed filter is indeed effective. The sine-wave appears clean in time domain, in spectrum domain the spurious free dynamic range (SFDR) is over 30 dB.

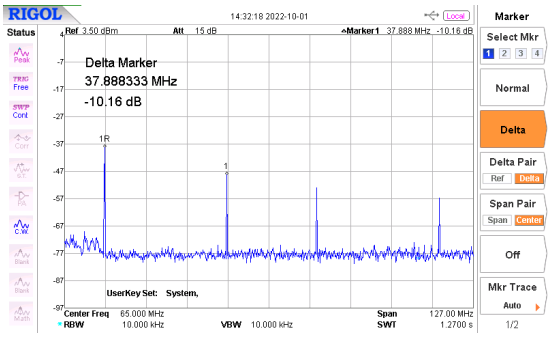


(a) Spectrum before filter

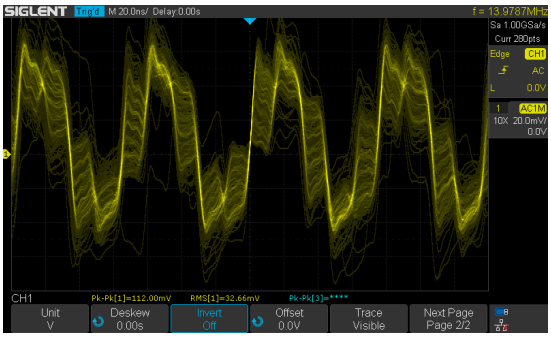


(b) Waveform before filter

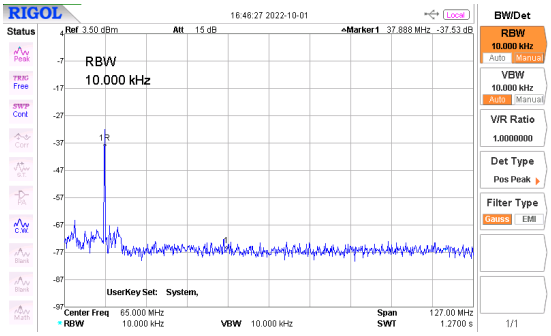


(c) spectrum after filter


(d) Waveform after filter

Figure 2.38: Singal from the DDS and test of the designed LPF on a real PCB

### 2.5.3 Transmit mixer

Having clean VFO signal that can span across different frequencies and constant IF signal containing desired modulation an RF mixer can be used in order to combine the two signals shifting modulated signal to a desired transmit frequency.

#### Choosing proper VFO range

As mentioned previously in conclusion to ladder filter design (see section 2) the shape of a home made ladder filter favors the rejection of upper sideband. However we want to create an upper sideband. This problem can be solved with a trick in second mixer that involves up conversion using higher range of the VFO.

Let's start with examination of how RF mixer works to understand this phenomena.

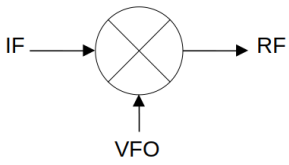


Figure 2.39: Diagram of RF mixer

Mixer produces sum and difference of the inputs. This sum can be described in the fig. 2.39 as:

$$RF = \begin{cases} LO + IF \\ LO - IF \end{cases}$$

Therefore if we want to create a 14 MHz signal with upper sideband in the output it is quite easy and intuitive. Such a spectrum is presented in fig. 2.40, in this diagram only fundamental signals with positive frequency are shown. In reality a mixer will produce also multiples of sum and differences (with lower magnitude) a theoretical operation would also produce negative frequency.

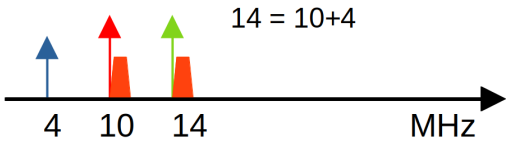


Figure 2.40: Ideal spectrum that shows up-conversion in a simple way

This case is easy to understand because up conversion does not flip a mirror of original modulation this lowers the necessary VFO to 4.0-4.35 MHz.

Another method uses the difference created by RF mixer. This method mirrors the IF therefore LSB has to be created by the filter and USB has to be rejected. This is a great benefit because the created filter has a much steeper slope at the upper side. Such a solution also puts VFO further from desired frequency making it easier to reject, sum of the signal is even higher in the spectrum so it is also easy to reject.

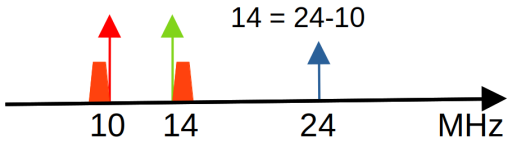


Figure 2.41: More complex solution improving sideband rejection

This means that for best performance of the SSB the VFO should have a range of 24.0-24.35 MHz to cover the 20 m band (14.0-14.35 MHz). However in presented experiments simpler scheme was used because of time constraints demonstrating worse case scenario.

For a physical realization of mixing a NE602 will be used not to extend the bill of material. This double balanced mixer can also be used as a normal mixer, schematic is shown in fig. 2.42

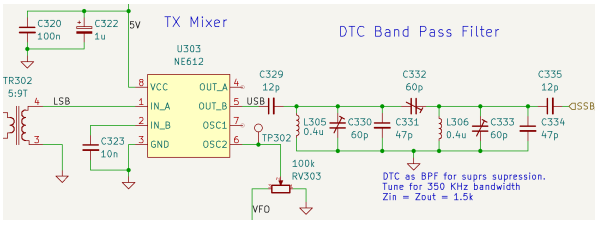


Figure 2.42: Schematic of TX mixer

### 2.5.4 Output band pass filter design and evaluation

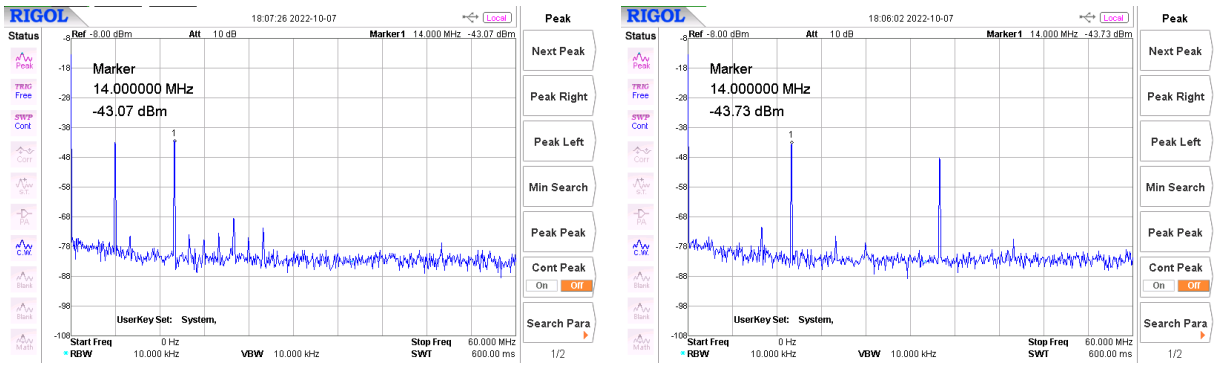


(a) 4 MHz LO scheme

(b) 24 MHz LO scheme

Figure 2.43: Signals from NE602 mixer for different VFO (LO) values and 10 MHz IF

Due to mentioned nature of the mixer at the output we get a lot of spurious signals that are mirror images of the desired signal, beside that LO and IF is also passed to the output. Output from a mixer shown in fig. 2.43.

It can be seen that the higher VFO scheme seems to produce an image that is easier to reject since the LO is much further apart (20 MHz instead of 4 MHz). 10 MHz IF is also visible although it is very weak. Still one should use a band pass filter in order to assure that only desired frequencies will leave the mixer.

Procedure for a band pass filter will be once again taken from the EMRFD book[6]. Typical topology for such application is a double tuned circuit. Naturally more stages can be used to create steeper response like in triple tuned circuit however our unwanted signals are far apart that selectivity of a DTC should be more than enough.

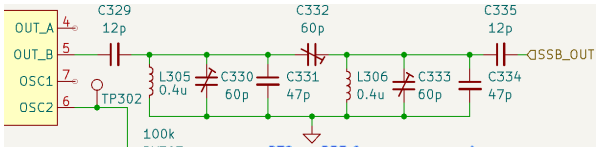


Figure 2.44: Schematic of double tuned circuit

The design will be conducted for the following parameters:

- Center frequency: 14.15 MHZ
- Bandwidth: 350 KHz
- Type: Chebyshev 0.25 dB ripple

For the design we again look at the table for the normalized values for Chebyshev filter. These values (q = 0.7154 and k = 1.779) come from the EMRFD book[6]. Next we need to pick an inductor value, book sugests some good starting values. Value of 0.4 $\mu H$ on a T37-6 core was chosen. Next using toroids.info website (`http://toroids.info/T37-6.php`) amount of turns was calculated given the desired inductance and core type.

After coil was wound with 0.37 mm enameled copper wire a precise ohmmeter (Fluke 8860A) was used to measure coil resistance in order to determine its Q factor at a 14.15 MHz frequency. Q of a coil can be calculated as:

$$Q_l = \frac{\omega L}{R_l} \tag{2.10}$$

Resistance was measured to be 0.072 Ω which translates to Q factor of 488. This is quite a high value which should make it steep. Knowing that the output impedance $R_O$ of the mixer is again 1.5k the values of

tuning capacitors can be calculated using equations:

$$\omega = 2\pi f_c \tag{2.11}$$

$$C_0 = \frac{1}{\omega^2 \cdot L} \tag{2.12}$$

$$C_{12} = C_0 \cdot \frac{k \cdot Bw}{f_c} \tag{2.13}$$

$$Q_E = \frac{q \cdot f_c \cdot Q_u}{Bw \cdot Q_u - q \cdot F_c} \tag{2.14}$$

$$C_E = \frac{1}{\omega} \cdot \frac{1}{\sqrt{R_o} \cdot Q_E \cdot \omega \cdot L \cdot -R_o} \tag{2.15}$$

$$C_t = C_0 - C_E - C_{12} \tag{2.16}$$

Using this series of equations the parallel capacitance was determined to be 302 pF and series capacitance was calculated as 14 pF. Because of unusual values several through hole capacitors were used in parallel alongside for capacitors that are in parallel with the inductors. Trimmer was used as a series capacitor to obtain the 14 pF, this value is important because as it was found out during tuning this value affects the bandwidth.

The double tuned circuit was assembled on the copper board and mounted close to the assembled SSB exciter board (see fig. 2.45).

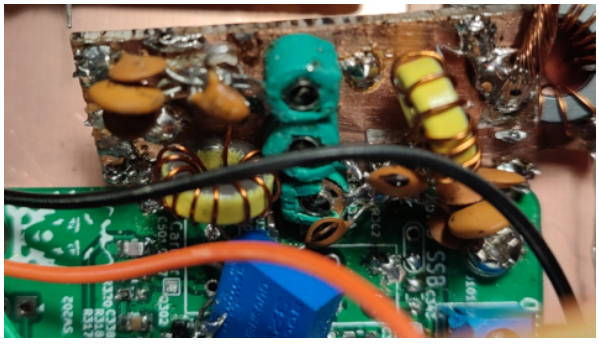

Figure 2.45: Assembled DTC

Created filter has an impedance of 1.5 k so the use of spectrum analyzer might skew a result of measurement especially when it comes to the ripple in the passband.
Instead of spectrum analyzer with tracking generator an oscilloscope was used with FFT function. The detector was set to maximum hold mode and the microcontroller was programmed to sweep the VFO. Because of the high input impedance of the oscilloscope (1M) the result should not be significantly affected by the measurement setup. Sweep was repeated many times in loop so that oscilloscope had opportunity to capture peaks of the signals. This created a response of the exciter for the wide frequency range.

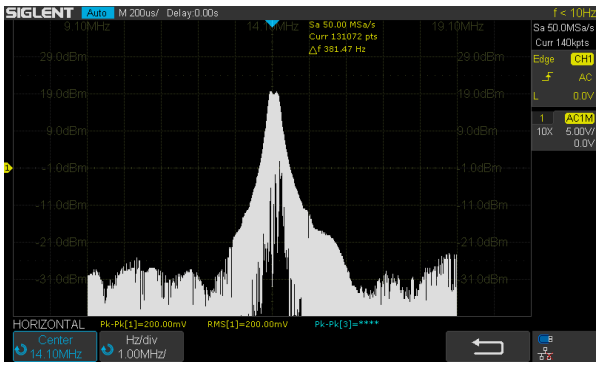


Figure 2.46: Frequency response output from the exciter

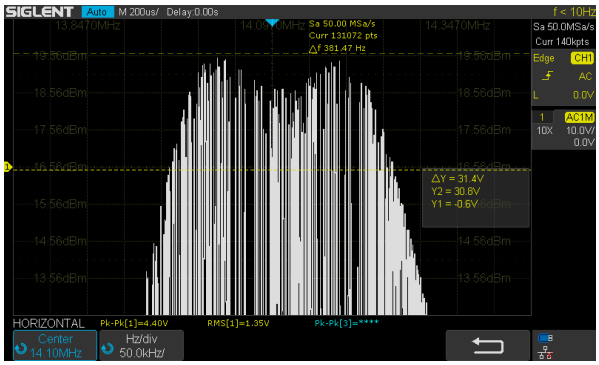


Figure 2.47: Frequency response output from the exciter

It can be seen in the fig. 2.46 that the spurious free dynamic range is more than 40 dB. This shows that spurious signals are indeed attenuated. Maximum values of magnitudes for frequency bins have created over time a shape of output filter. Setting the span to 50 KHz per div (see fig. 2.47) shows that the ripple in the pass band is about 0.8 dB instead of 0.25 dB, so more than we desired. This is still not a bad result and to reach a full conclusion a more in depth check of the matching transformer of the DDS should be carried out with a proper

equipment. The resulting ripple might be not because of the filter but because of the error stacking of poor DDS to LPF match, mixer response and then finally the DTC match and ripple. Result is however sufficient for operation, the -3dB bandwidth is approximately 300 KHz which is sufficient to cover the voice portion of the 20 m band as desired.

After that a Spice simulation was made for two double tuned circuit filters. One used the normalized values k=0.7071, q=1.414 for the Butterworth filter. Second filter used values k=0.7154, q=1.779 for 0.25 dB Chebyshev as for the filter that was assembled in the real circuit.

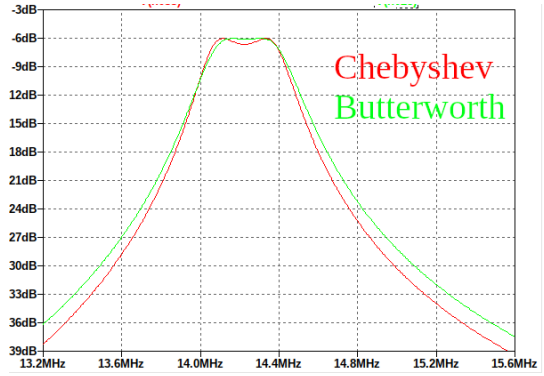


Figure 2.48: Comparison of Chebyshev and Butterworth DTC in LTspice

In the figure 2.48 it can be seen that the filter described by Butterworth polynomial is very flat in the passband but it also has a less steep roll off. The Chebyshev on the other hand has a ripple of 0.6 dB, so more than calculated 0.25dB. This Chebyshev simulation seems to correlate closely to our assembled filter.

## 2.6 Test with the receiver

At this stage the SSB signal is ready for amplification. However it is worth to check if the modulation is correct and if significant distortions are present. For that a software defined radio (SDR) will be used.
Instead of table top radio a USB dongle with RTl2832u chip will be used with GQRX software. This dongle uses quadrature sampling and with GNU Radio it demodulates received signals. Types of modulation include single sideband. The limitation is that it works from 25 MHz therefore another mixer with 16 MHz oscillator input was used as an up converter so that signal can be received on 30 MHz.

After turning on the exciter and speaking into a microphone signal was observed on the waterfall.

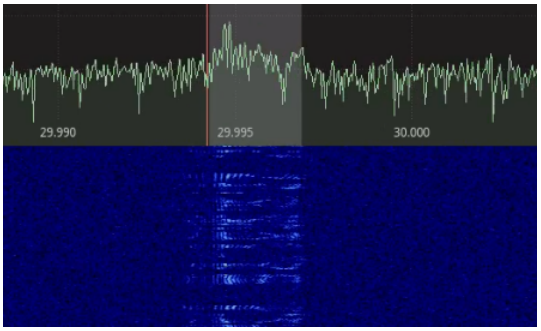


Figure 2.49: Waterfall view of the SSB signal generated by the exciter

In the figure 2.49 the vertical axis is time, horizontal is frequency and brighter color indicates a magnitude of signal at this time and frequency. This plot is called waterfall and is a useful feature in SDR receivers for finding stations, determining their bandwidth and overall spectral quality. Intensity of the signal is present when words are spoken into a microphone. The carrier is very weak (signal adjacent on the left). When no audio signal is present the signal output together with the carrier practically disappears which is good. GQRX also demodulates the audio, example FFT of received audio is shown in the upper part of fig. 2.49, the frequency roll off above 3 KHz, this is partially because of the receiver filter but also because the exciter does not exceed the 3 KHz bandwidth which is seen on the waterfall. The waterfall can be seen as a wide band receiver while demodulation takes only the signals within the filter range. Listening to the audio some distortion is present however the voice is understandable and quite clear. It is certainly enough for a 5 report in amateur radio report methodology (where 5 is the highest report).

## 2.7 Linear amplifier

Having examined the SSB signal we are ready to amplify it so that it can be later on delivered to an antenna and be radiated.

### Theory and necessity for linearity

Amplifier for SSB signal should be highly linear. By definition, a system is linear if it satisfies the superposition principle for all inputs at all time. That is has the given property:

- Additive: $f_(x_1) + f(x_{21}) = f(x_1 + x_2)$
- Homogeneity: $a \cdot f(x) = f(x \cdot x)$

This means that no new signals are created other than sum of the input signals and their scaling. This is important because non linear amplifier could act as a mixer adding new signals like harmonics or intermodulated signals. This effect will be closely investigated because spurious signals might affect other users of the radio spectrum and they also decrease efficiency of our transmitter since power density is lowered.

### 2.7.1 Pre-amplifier

Since the output signal from the exciter is very small it needs to be amplified by multiple stages. First two stages are directly taken from the Lichen transceiver that was presented in EMRFD[6].

First stage consists of two amplifiers based on 2N3904. These small signal amplifiers work in class A for low distortion, as a biasing emitter feedback is used. This method of bias uses both emitter bias and collector bias for improvement of stability. The collector feedback improves stability independent of $\beta$ because if the collector current increases the voltage from ground to collector decreases this in turn reduces the base voltage. This negative feedback reduces current flowing to the base limiting the collector current hence keeping the Q point stable.

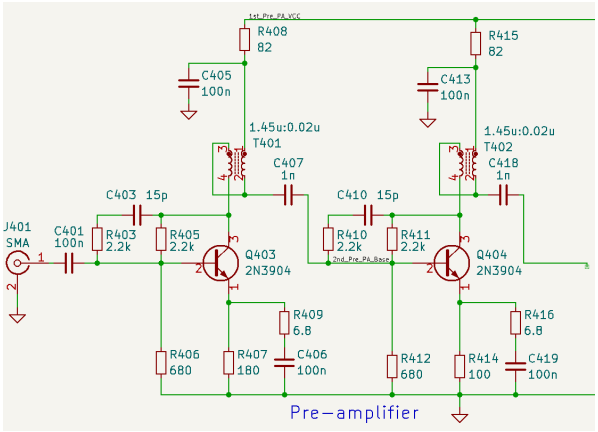


Figure 2.50: Pre-amplifier stage from Lichen transceiver

The emitter resistor network is used to set the collector and emitter current. Note that the DC point is set by two resistors in series. One smaller resistor is for gain degradation, this is done so that the RF signal is not just bypassed from emitter to ground.

These stages do not provide high gain or power, they provide however 50Ω input impedance and are fairly linear. Input to the amplifier is coupled by a capacitor, inter-stage coupling is also done by capacitor but with bifilar transformers for impedance matching. This stage should produce around 150 mW of power which is enough to drive medium power transistor.

Next stage is a medium power transistor. Here the same type of bias and negative feedback was used. The 2N3866 transistor was changed to a more obtainable and less obsolete 2SC2314 which was refurbished from an old CB radio. Because of difference in Beta a base to ground resistor needed to be increased from 680 $\omega$ to 810 Ω. This increased the base voltage and put this stage also in A class.

Collector loading was also changed for this stage. Instead of next bifilar autotrans-

former for impedance matching a single inductor was used. We can assume for now a purely resistive load that should be seen by a collector of a common emitter NPN transistor amplifier. Typical value for such load (between supply rail and collector) should be 250 Ω. For an RF amplifier we should replace this resistance with reactance, equal inductor that will present such 'resistance' at the lowest operating frequency of the transmitter cal be calculated using formula:

$$X_L = 2\pi f L \tag{2.17}$$

$$L = \frac{X_L}{2\pi f} \approx 2.9\mu H \tag{2.18}$$

Again using toroids.info a value of turns for FT37-43 was calculated and 3 turns were wound on the toroid.

### Driver

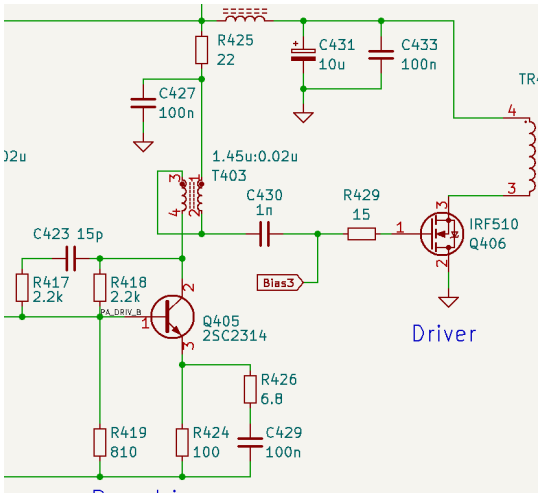


Figure 2.51: driver and final stages from lichen transceiver

As a drive a MOSFET is being used. Using an IGBT device is not a new concept since LDMOS devices are popular for a high power stages in RF amplifiers however used MOSFET was not designed for high frequency operation. IRF510 is a popular switching device often used in power converters. However some amateur RF designers proven its usefulness as RF power transistors even at 14 MHz.

Use of the MOSFET requires a different bias network since this device is voltage driven. For efficient yet still linear operation this stage is an AB class. Comparison of MOSFET bias methods in RF amplifiers was presented by Iulian Alin Roșu YO3DAC in his paper "Bias Circuits for RF Devices"[20]. In class AB the gate voltage should be put a bit higher above the threshold voltage so that some current is flowing even in idle operation.

For bias voltage a 5 V regulator and a potentiometer is being used as a voltage divider. Tap of the potentiometer is connected by a 10 k resistor to a gate of MOSFET, this provides a high impedance so that bias voltage can be decoupled by a 100 nF capacitor. Different values of idle collector current were checked and output power was observed. YO3DAC provides extensive solutions for closed loop MOSFET biasing with regulation schemes.

At this stage no compensation for thermal effect is applied, however thermal runaway is unlikely since the driver does not operate with high power. This stage needs to produce approximate 1 W of power while the Lichen presented in EMRFD can produce up to 5 W.

Drain is loaded with a transformer with 2:3 turns ratio. The core used for best coupling and lower loses is of a binocular type and is also made out of type 43 material (BN43-302). Driver and preamplifier stages were assembled on a copper board using Manhattan style construction as a prototype (see fig. 2.52). SMA connector was used for the input and output. This low power amplifier was connected to a 50 Ω dummy load for a test.


Figure 2.52: Low power amplifier

Before further testing the input impedance of the amplifier needed to be evaluated so that input power could be calculated from the voltage set on the signal generator. For that a vector network analyzer (VNA) was used. VNA can plot complex impedance across frequency span on a Smith chart, in the figure 2.53 measurement of amplifier's input is shown.

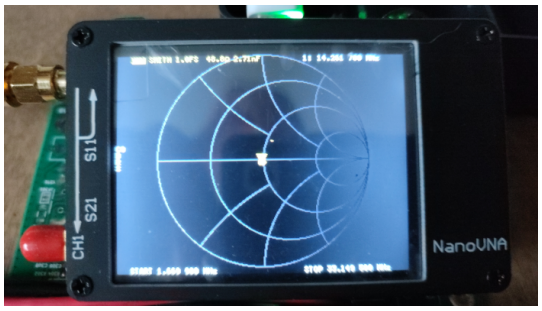


Figure 2.53: VNA measurement of amplifier's input impedance

Impedance seen at 14.1 MHZ is 48 Ω which is very close to 50 Ω, this impedance is almost constant across the whole shortwave spectrum.

Knowing the peak to peak voltage of sinusoidal signal across the input and input impedance, power can be calculated in dBm using formulas:

$$V_{rms} = \frac{1}{2\sqrt{2}} \cdot V_{pp} \tag{2.19}$$

$$P_{dBm}(V_{rms}) = 10 \cdot log_{10}\left(\frac{V_{rms}^2 \cdot 1000}{R_{IN}}\right) \tag{2.20}$$

Voltage from the generator with 50 Ω output was increased in 5 mV steps from 5 mV to 50 mV (-42 dBm to -16 dbm). The gain test was made for two quiescent drain current values: 20 mA and 40 mA and for two drain voltage supplies for the IRF510 stage: 12 V and 24 V. Other stages were supplied by 12 V in all 4 tests. Input impedance of the amplifier was 48 Ω close enough to the generator's output to assume 1:1 match.

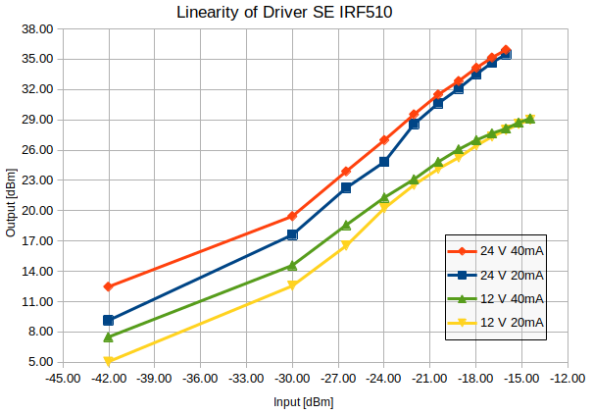


Figure 2.54: Gain for the IRF510 single ended amplifier, test of assembled circuit

Graph in the fig. 2.54 shows the gain of the assembled stages. This tests both linearity of the stages and output power. Ideally a linear amplifier could be represented by a simple y(x) = x line. Real amplifier however will introduce some compression at higher input. Point where real output power decreases by 1 dB in comparison to extrapolated linear region is called compression point. We can see that our low power stages do not reach significant compression for drain voltage of 24 V however at 12 V some compression starts to be visible at -15 dBm of input.

However circuit performs quite linearly, measurement for lower input levels such as -42 dBm might be skewed because of noise in picked by the oscilloscope probe. Increase in quiescent current had slight improvement on linearity and made only marginal difference in maximum output power.
For the 24 V system 37 dBm of output power can be obtained which is equal to 5 W just like the authors of Lichen claimed. For 12 V 29 dBm were measured which is 0.8 W but even this value might be enough to drive the final stage.

### 2.7.2 Final stage

Final stage was inspired by QST article from March 1999 by Mike Kossor WA2EBY[15][16] this amplifier uses two IRF510 MOSFETs in push pull configuration and was originally based on another QST article from January 1993 by AA3X. Authors claim that more than 30 W is possible with both amplifiers. WA2EBY is however a worthy notion because it improves output power for the higher frequencies.

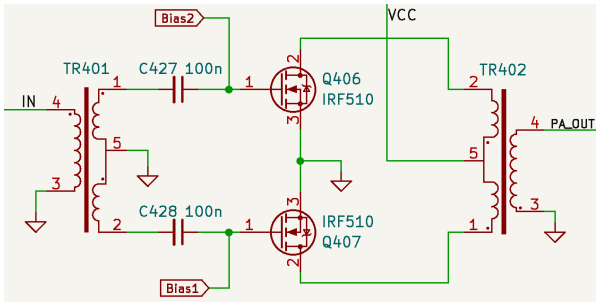


Figure 2.55: Schematic of final stage

VCC is a supply voltage that needs to be well decoupled, for that two 100 nF and 1 uF capacitors in parallel are used, 50 V or higher rated capacitors should be used here because of high voltage that might be induced. This rail also passes through an RFC which is made out of 14 turns on a FT50-43 core and is also decoupled on the other side. On both sides of RFC a 1 uF capacitors server a two purposes. First is that they prevent a series resonance between coil and 100 nF capacitors. The 1 uF capacitors have higher ESR so the oscillation is damped. This effect and solution to it was presented in Analog Device's application note AN-583[3]. The other reason is a parallel resonance between small and large capacitors that are also on the board in order to prevent voltage from sagging since SSB can cause sudden spikes in current.

#### Bias and thermal protection

Another consideration is bias network. Final transistors will get much warmer than a driver. With a BJT transistors increase in temperature causes decrease in emitter-base voltage and thus increase base current which leads to more collector current this in turns causes more heat dissipation. This is a description of thermal runaway. According to YO3DAC in his paper on RF amplifiers[21] MOSFETs have negative thermal coefficient and thus their transcodnuctance and drain saturation current decreases with temperature.

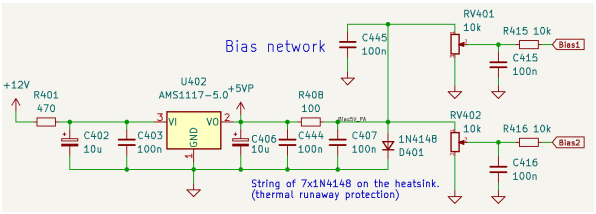


Figure 2.56: Bias network for the finals

However some MOSFETS were still damaged during the tests while continuous high power was drawn from the amplifier. As a solution a bias network will be improved with a series 100 Ω resistor and a string of 7 parallel forward biased diodes with cathode side connected to ground. Thermal effect decreases voltage across semiconductor junction as the temperature increases. This means that a string of diodes with resistor will output roughly 4.9 V ($4 \cdot 0.7$ of forward voltage) at room temperature, but when temperature increases the string of diodes with resistor starts to act as a temperature dependent voltage divider. This effect was also tested in Spice software and for an increase from 20 $°C$ to 80 $°C$ a voltage drop of 0.45 V was observed. This is enough to lower the bias voltage of MOSFETs to a point where the drain current will be effectively shut off. Transistors also have to be mounted to a significant heat sink with isolating pads and non conductive thermal compound. During testing forced airflow from a 90 mm fan was used at all time.

### Push-Pull configuration

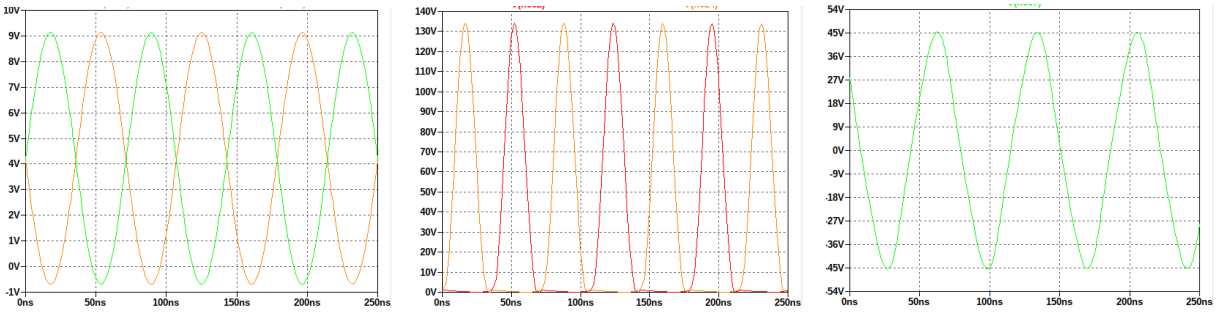


(a) Signals at the gates (b) Signals at the drains (c) Combined signal

Figure 2.57: Signal flow through a push pull MOSFET amplifier simulated in LTspice

Input transformer is an output transformer from the Lichen but with modified secondary winding. Secondary winding needs to divide the signal into two signals being in 180° phase to each other. This is done because in class B conduction angle is 180° in push pull one transistor conducts during positive half cycles and second transistor conducts during negative cycles. Output signal is then combined in an output transformer, this poses risk of crossover distortion. We can observe this effect in simulation. Notice that a combined output in figure 2.57c is not a perfect sine wave.

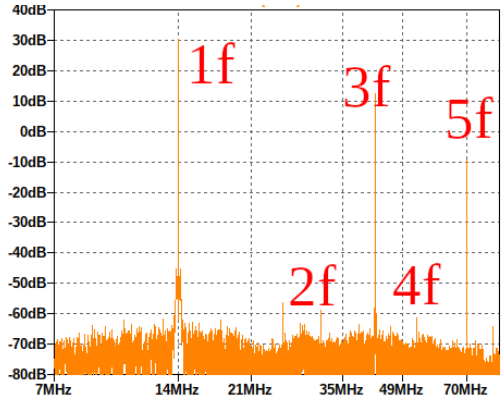


Figure 2.58: Simulation of final stage

The B class amplifier improves efficiency, the push pull configuration can deliver 3 dB more of power for the same conduction angle[21] and it also causes the even order harmonics to cancel out (2f, 4f, 6f)[15]. This is important because first even harmonic is difficult to suppress in the output because it is close to a fundamental signal. This effect is shown in fig. 2.54 where in Spice simulation the final stage was driven so that 1 W was observed at the output.

The fundamental signal is at 14 MHz, even harmonics at 28 MHz and 56 MHz are greatly attenuated while harmonics at 42 MHz and 70 MHz are in their expected magnitudes.

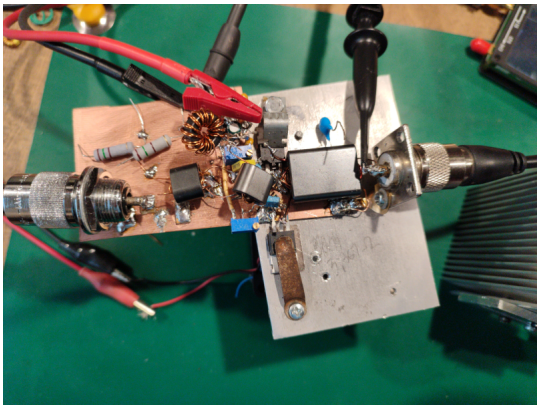

Figure 2.59: Assembled final stage

After satisfying simulation a prototype of the amplifier was built on copper board. TR402 was wound on a BN43-3312, larger binocular core was necessary here to handle the adequate power. Smaller core such as previously used BN43-302 could easily get saturated and with high temperature it would loose its ferromagnetic properties. Primary side consists of a half turn for each side using enameled wire of 1 mm diameter while the secondary side has three turns made with 0.37 mm diameter enameled wire. The primary side presents a very low impedance therefore we higher current

will be present. Secondary side will be transformed to higher voltage and lower current. It is also important to note that higher diameter is also important because of the skin effect which causes RF energy to flow on the outside of the conductor. Some RF transformers are made using small tubes to increase surface however here such materials were not available at that time.

### 2.7.3 Low pass filter

Even though we were able to cancel out even harmonics in simulation, reality does not always conform to simulation, not to mention the magnitude of odd harmonics. Therefore a low pass filter has to be designed. The design process follows the same steps as it was presented in section 2.5.2. This time however the filter is designed to be doubly terminated by 50 Ω, the cut off frequency was set to 16 MHz. Necessary value of the inductors was calculated to be 0.62 uH and the capacitors were calculated to be 250 pF. Toroids were wound using 0.37 mm diameter enameled wire on a T37-6 toroidal coil. Material used for this toroid has a permeability that makes it suitable for high Q inductors below 1 uH. 14 Turns were wound on each toroid.
Capacitors used for low pass filter should withstand peak to peak voltage higher than 200 V. Lack of proper capacitors made with X5R, X7R NPO dielectric has forced use of 250 V capacitors dedicated for mains filtering. Value 220 pF and 470 pF were the closest possible values on hand. Even though this is not perfect these values can make a half wave filter. Half wave filter uses capacitors with the same values on the input and output of the filter and double value in the middle between the inductors.

This experimental method was tested using vector network analyzer.

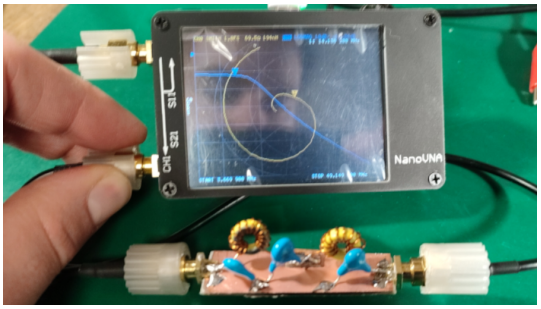


Figure 2.60: LPF test with VNA

In the figure 2.60 two plots can be seen, Smith chart with yellow line and magnitude plot as a blue line. From the Smith chart it can be read that the filter is closely matched to 50 Ω up to 16 MHz, above that impedance rises. This is a proper behavior of a low pass filter. On the magnitude plot it can be seen that we would normally see on a spectrum analyzer with a tracking generator. Spectrum analyzer was used for measurement of insertion loss.

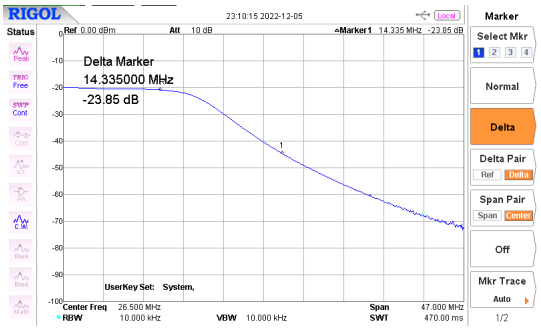


Figure 2.61: LPF test with SA

Looking at the insertion loss at the highest frequency of 20 m band (14.35 MHz) we are losing 0.85 dB. This result is not quite good. Simulation in spice was made to determine potential loss with ideal components with the same capacitance and inductance and it was determined to be 0.38 dB. Further investigation should take place to determine whether cable, connectors and coils imperfection affect the loss so much or if the capacitors used cause loss of signal. Either way such loss will not affect power output to a significant degree.
In terms of spurs suppression at 28 MHz we have attenuation of 23.8 dB at 42 MHz we have more than 30 dB of attenuation so there should be no problems with FCC compliance.

### 2.7.4 Output measurements

For a power measurement a dummy load was connected to an amplifier. Dummy load presents almost perfect 50 Ω impedance across wide frequency spectrum because it uses a special low inductive resistor made by Florida RF. It can also dissipate up to 250 W being mounted to an adequate heat sink. Dummy load was made in a way that allows low inductance connection of the X10 probe of an oscilloscope. Directional coupler or set of attenuators with suitable parameters for this power measurement was not available. Oscilloscope presents high impedance so the front end will not skew results or be damaged by the excessive power from the amplifier.

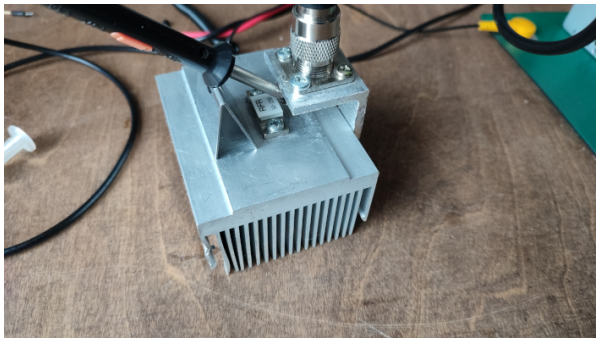

Figure 2.62: Dummy load

The output of the low power section with single ended IRF510 driver was connected to a push pull final with two IRF510s, voltage supply of this section was connected to 13.9 V supply (common value in amateur radio). Power was increased at the input and output was measured. The quiescent current of the final MOSFETs was set at 30 mA for each. In the first test the amplifier was run with no low pass filter, the output was observed for the highest power output. Result is presented in fig. 2.63. Fundamental signal reached 46.4 dBm which is 43 W. This is a lot of power for such an amplifier. This setting is however not very stable with total current consumption of 3.3 A and 28 V DC for longer run the MOSFETs sustain fatal damage due to excess in peak drain voltage. It is however worth to examine the harmonics. Even first harmonic (28 MHz) is attenuated by 20 dB while the second harmonic (42 MHz) is only 10 dB below fundamental signal. This is a worst case scenario where the amplifier produces most spurious signals and for such a case designed low pass filter should have no problems with making our amplifier FCC compliant (-43 dBc required for mean output).

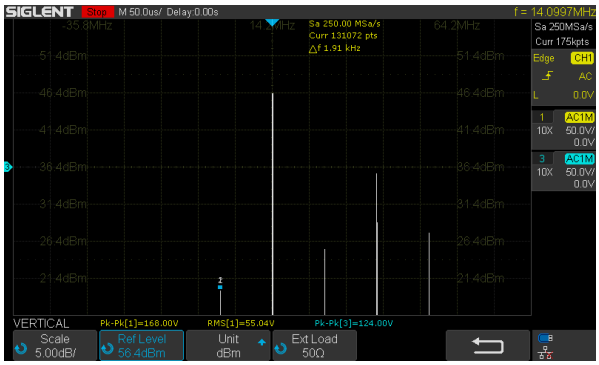


Figure 2.63: Output of PA without LPF

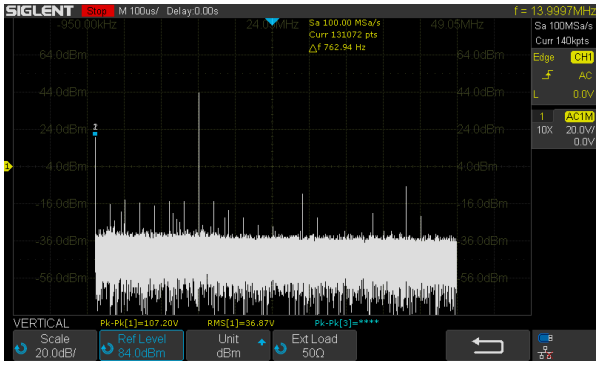


Figure 2.64: Output of PA with LPF

It can be seen in the figure 2.64 that low pass filter manages to keep the spurious signals well below the fundamental signal. The 28 MHz harmonic is 55 dB below and 42 MHz harmonic is about 50 dB below. One has to remember that this measurement setup is very limited because of the poor dynamic range and high noise of the oscilloscope.

After the low pass filter was connected to the output a simple test was conducted in order to establish the relation between gain and supply voltage for the final transistors. Input was increased from signal generator and power was measured, for each run a different value of supply voltage was set.

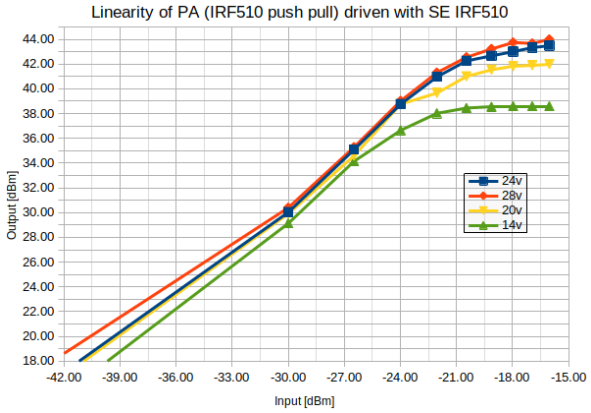


Figure 2.65: Gain chart for the assembled amplifier

In the fig. 2.66 it can be seen that with 14 V of supply the amplifier puts out 8 W. For 20 V we see significant increase to 42 dBm (15.9 W) while between the 24 V and 28 V the difference is negligible probably due to saturation. In fact for 28 V drain voltage during operation the source to drain voltage was very close to the maximal value of 130 V from the data sheet. Maximum achieved 44 dBm equates to over 25 W. With less insertion loss and better transformer winding a 45 dBm (over 30 W) is a definite possibility. Results for -42 dBm are most likely skewed by noise in the system, this limitation of the test setup impacted the next measurement where input level started with -30 dBm.

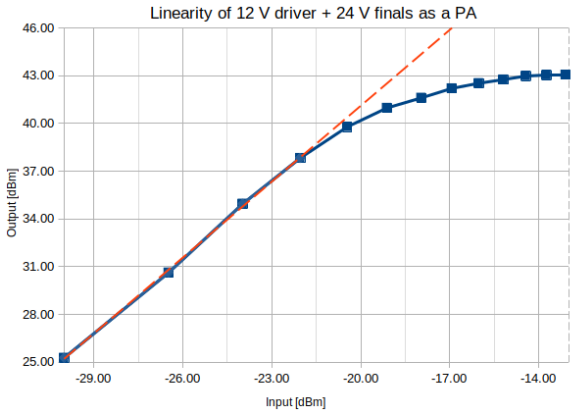


Figure 2.66: Compression point and linearity chart

Even though amplifier reaches 20 W output power with a low pass filter it is important to remember that the linear region does not cover the whole span of input power level. This means that the linearity is not fulfilled because the homogeneity principle is not fulfilled for all input. In order to claim that amplifier as a linear we should specify maximum input level. For that a compression point is used, it is a theoretical point for which real output power level drops 1 dB below the expected extrapolated level from the linear region. In fig. 2.66 a trend line was plotted to extrapolate the linear region, looking for an input level where power deviates by 1 dB from expected output. For level of -20 dBm output power is 40 dBm so only 10 W. This is still satisfying result and fits our goal of very good linearity and output power.
Driving amplifier into non linear region produces much higher power but at a cost of distortion which should be avoided.

Next important test in order to determine linearity involves the measurement of second and third harmonic and their hypothetical intercepts with fundamental power level. Iulian Rosu describes intermodulation products in his paper on RF Power Amplifiers[21] as a sum and differences of fundamental tones of the amplifier and its harmonics. In short some non linear effects are seen if two or more tones are input into the amplifier allowing for intermodulation of those two signals. Because of the sum and difference phenomena this is also known as AM-AM distortion. Unfortunately at the time of writing measurement setup was not sufficient to conduct such a measurement due to lack of good dual tone source.

Robustness and effectiveness are another important aspects of a power amplifier. Thermal sensor (18B20) was wedged to the top of the TO-220 package of one of the final IRF510s, the temperature was read every 500 ms for a period of 400 s (6.6 minutes). Two constant power output levels for sinusoidal signals were investigated and a plot was made from gathered data.

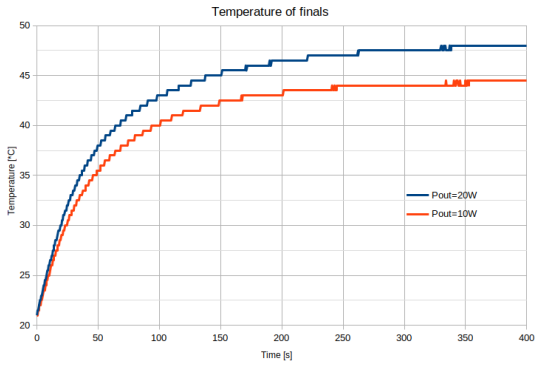


Figure 2.67: Temperature of finals over time

With output power of 20 W into a 50 Ω load amplifier reaches a temperature of 48°$C$. Observed curve resembles a logarithm and it flattens out after a certain time not exceeding 48°C. Test for half of the output power shows that as expected the temperature rises to a lower value of 44.5°C. This is a satisfying result because we have shown before that operating well beyond 10 W introduces non linear gain which is unwanted and we know from the IRF510 data sheet that maximal operating temperature is 145°$C$. Measured temperatures over this long period with CW output are enough to ensure robust operation in normal conditions. In the next test RF output power level was increased and DC power consumption was monitored.

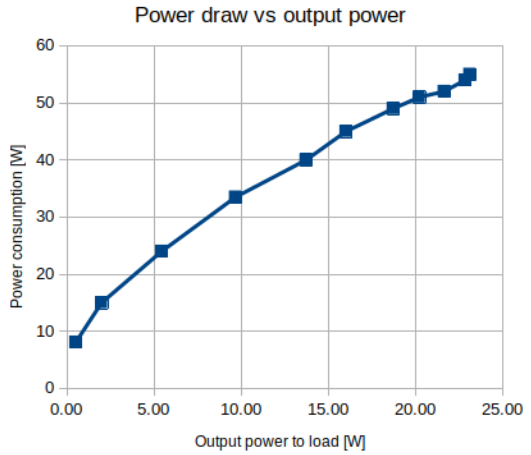


Figure 2.68: DC power draw for given RF output

From the fig. 2.68 it can be seen that DC input power increases linearly. The efficiency is higher for the higher output levels, probably due to the fact that bias of A class stages takes significant power in comparison to low output levels. For example for 5 W output the efficiency is only 23% while for 20 W it reaches 40% which is a decent result for this class of RF amplifier.

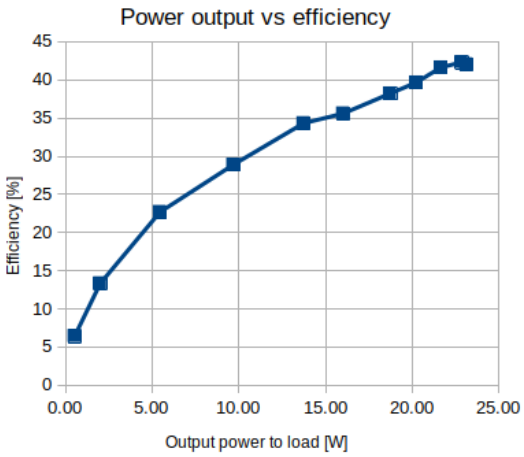


Figure 2.69: Efficiency vs output power

### Output switching

Mosfet controlled by a transistor is switching on power to the amplifier sections. Relay is used to connect the antenna to either the amplifier or to a pass-through connector, that way transmitter can be used alongside a receiver to create a full station. In such a case receiver has to be protected from RF generated by the final amplifier. First stage of protection is grounding the receiver by a second relay before the amplifier is energized. In order to prevent excessive RF induction to the receiver two diodes are connected backwards in parallel in order to create a simple clipping circuit. This switching and protection circuit was inspired by Radio and Electronics Cookbook[1].

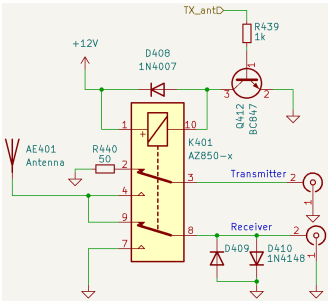


Figure 2.70: Antenna relay circuit

# Chapter 3

# Mechanical design

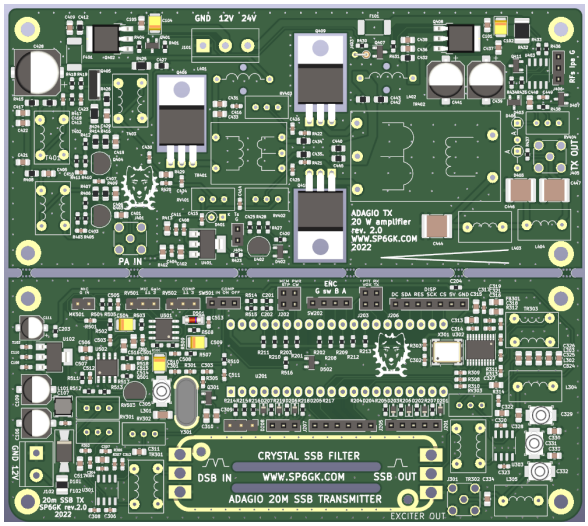


(a) Front of the PCB

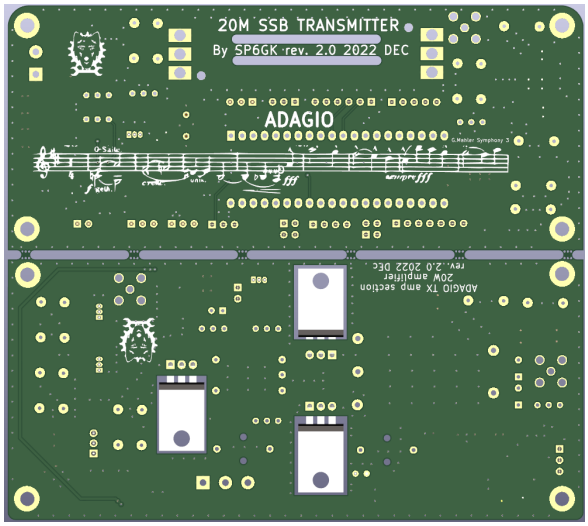


(b) Back of the PCB

Figure 3.1: Device is split into two boards that can be penalized.

## 3.1 PCB

Device uses a two layer PCB design with all components being mounted on the front side in order to minimize the cost of assembly. All components except for connectors, coils and potentiometers are in SMD packages to minimize form factor. SSB filter is a separate PCB so that either 4 or 8 crystal filter can be fitted. This also allows experimenter for creation of one good filter and exchanging it between prototypes.

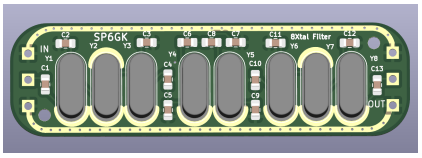


Figure 3.2: 8 crystals version of SSB filter

Beside SSB filter transmitter uses two PCBs, one for the power amplifier and one for the exciter. PCBs can be easily penalized which in figure 3.1 where mouse bites were used to create small panels.
Front copper layer was via stitched with back layer which is mostly a ground plane. TO-220 packages were mounted horizontally in order to mount them to a heat sink and also to stop them from mechanical resonance due to natural frequency of resonance. Thickness of 1 mm for the PCB is recommended in order to lower thermal resistance of top layer to bottom layer of the amplifier board so that heat can spread more easily. Given low frequency and manageable temperatures FR4 material was used. PCB trace width is no smaller than 10 mils.

As a larger project the transmitter was named Adagio to indicate a slow but in depth process of evaluation for each stage. Back silkscreen of the exciter board features a music line from the last movement of Mahler third symphony.

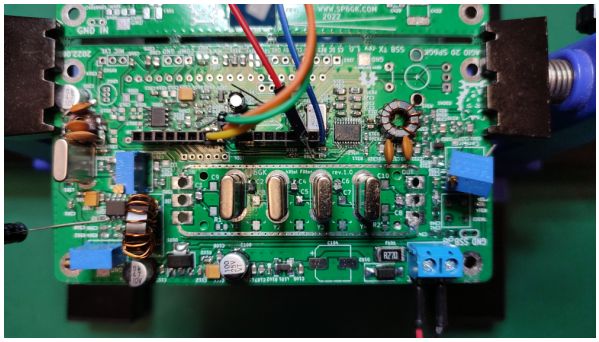

Figure 3.3: Assembled exciter PCB, only prototype revision was assembled

Bill of materials (BOM) was created using KiCad plugin and is attached in a form of a HTML code that can be viewed and be interacted with in a web browser.

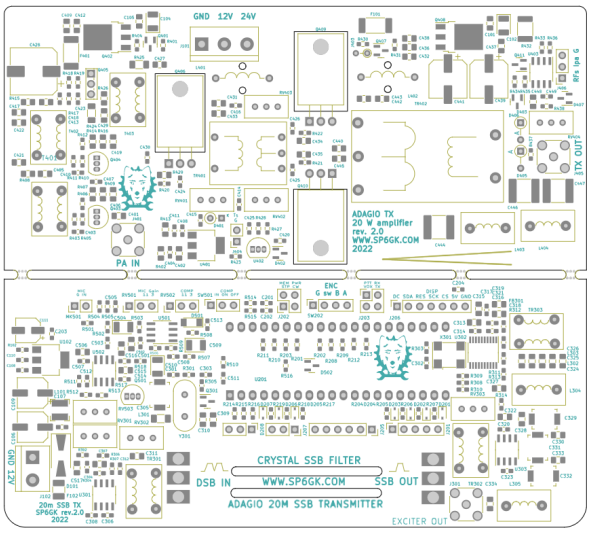


Figure 3.4: PCB assembly diagram

## 3.2 Case

Case of the transmitter is a re-used audio amplifier case. Front panel was designed in FreeCAD and was 3D printed in PLA. Additional space for the potentiometers allows for a conversion into a transceiver. VFO knob was also designed and 3D printed. Frequency, output power and standby status are displayed on a 1,8" 160x128 TFT display. Microphone is connected to a five pin aviation style connector. On the right side analog meter can be used for output power measurement using RF detector circuit.

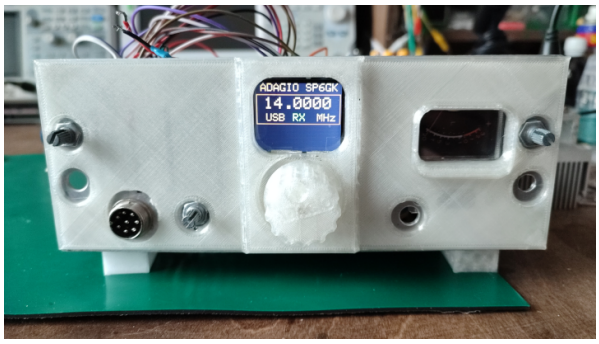


Figure 3.5: Front of the transmitter

Inside of the unit is split into two sections with two layers each, left side houses the SSB exciter and band pass filter, the right side houses the power amplifier and output filters. Front panel holds a module with display, potentiometers and encoder for the VFO. There is also space for some additional boards next to audio input.

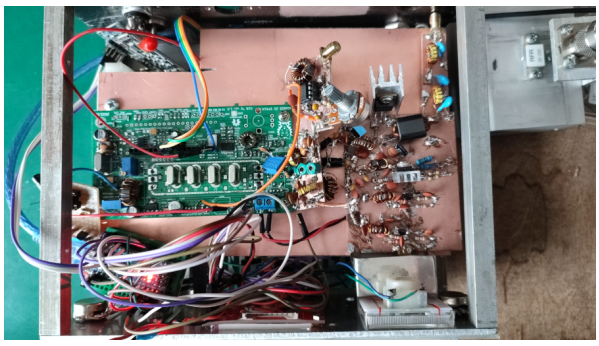

Figure 3.6: Transmitter during assembly

# Chapter 4

# Conclusions

Design of a whole RF chain for a single sideband transmitter was shown. Presented work expanded typical amateur radio construction of analog transmitter by addition of audio compressor which limits the dynamic range of audio signals but improves signal to noise ratio of transmission.
Working of Gilbert cell was explored and two active double balanced mixer circuits were compared in frequency domain in order to determine carrier suppression and spurious free dynamic range.

Then comparison of two methods for crystal's motional parameters calculation and subsequent simulation has shown that it is important to choose proper crystals from larger batch in order to create a good SSB filter. Some home made projects recommend setting of local oscillator to a given frequency and choice of filter tuning capacitors without consideration for variations in crystal's motional parameters due to manufacturing process. However model of a crystal based on G3UUR method of indirect motional parameters measurement has shown that using basic apparatus it is possible to precisely design a crystal ladder filter.

Two schemes of variable frequency configurations were shown and explained. Even though a simpler scheme with 4 MHz VFO a SSB signal was observed and was properly received using software defined radio. Carrier suppression was on a good level below 40 dB, lower sideband suppression was measured as 23 dB for 1 KHz signal which is not a good result. However, a method of proposal with positive results from simulation was proposed. Measurements have shown that crystal filter has steeper slope on the upper side and this can be used to our advantage with different VFO frequency that still allows for obtaining of 14 MHz output.

Main methods for low pass filters and band pass filters from "Experimental Methods in RF Design"[6] were used and were shown to be very effective both for output low pass filter and DDS reconstructive low pass filter as well as for a transmit mixer band pass filter.

Linear power amplifier demonstrated interesting use of cheap IRF510 power MOSFETs in RF amplification. Special care was taken during testing. Gain plots were created for different quiescent current and supply voltages. Compression gain and output power in the linear region was measured. Amplifier can produce up to 12 W in the linear region and PEP is approximately 30W. Unfortunately dual tone and IMD measurements were limited due to a measurement setup.
However harmonic measurement for single tone was conducted and amplifier meets the FCC requirement of -43 dBc suppression of spurious signals for mean power.

Overall this exercise has shown good practices when designing a communication transmitter for analog modulation like SSB. Designed device is a good basis for further experiments and development which is at the core of amateur radio as a hobby.

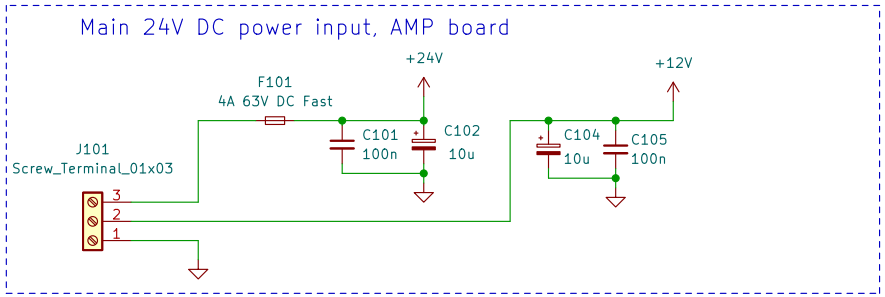


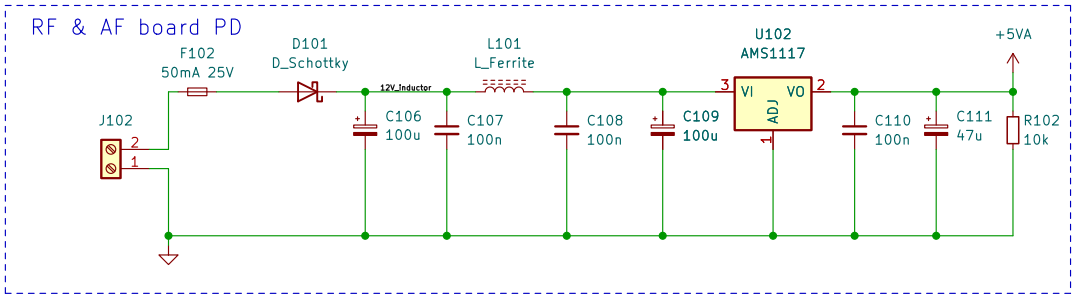


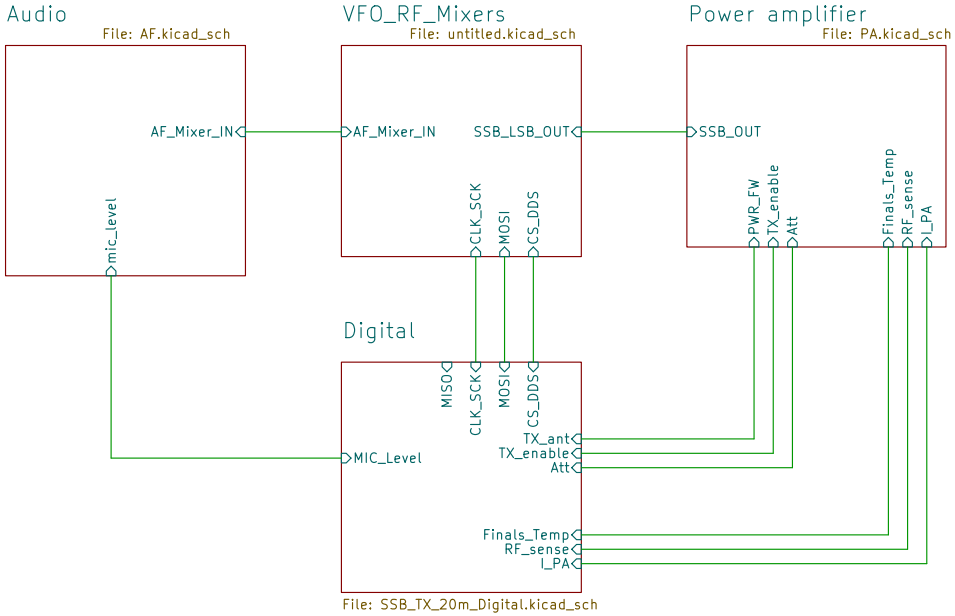


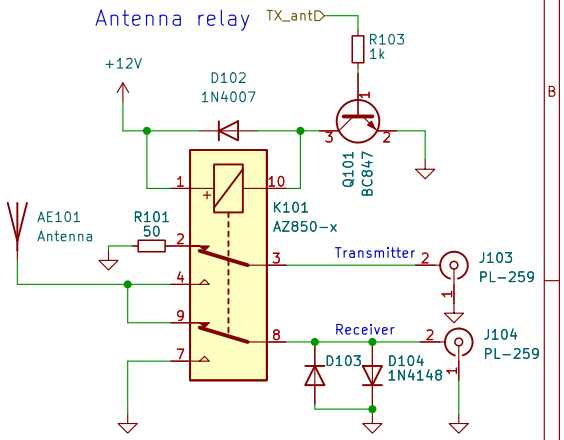


block diagram for hierarchical schematics
5V analog and 5V digital rails
12V input

**Grzegorz Krupa**

Sheet: /
File: SSB_TX_20m2022_hierarchical.kicad_sch

***Title: SSB TX Power distribution and block diagram***

| Size: A4 | Date: 2022-05-09 | **Rev: 1.0** |
|---|---|---|
| KiCad E.D.A. kicad (6.0.9) | | Id: 1/5 |

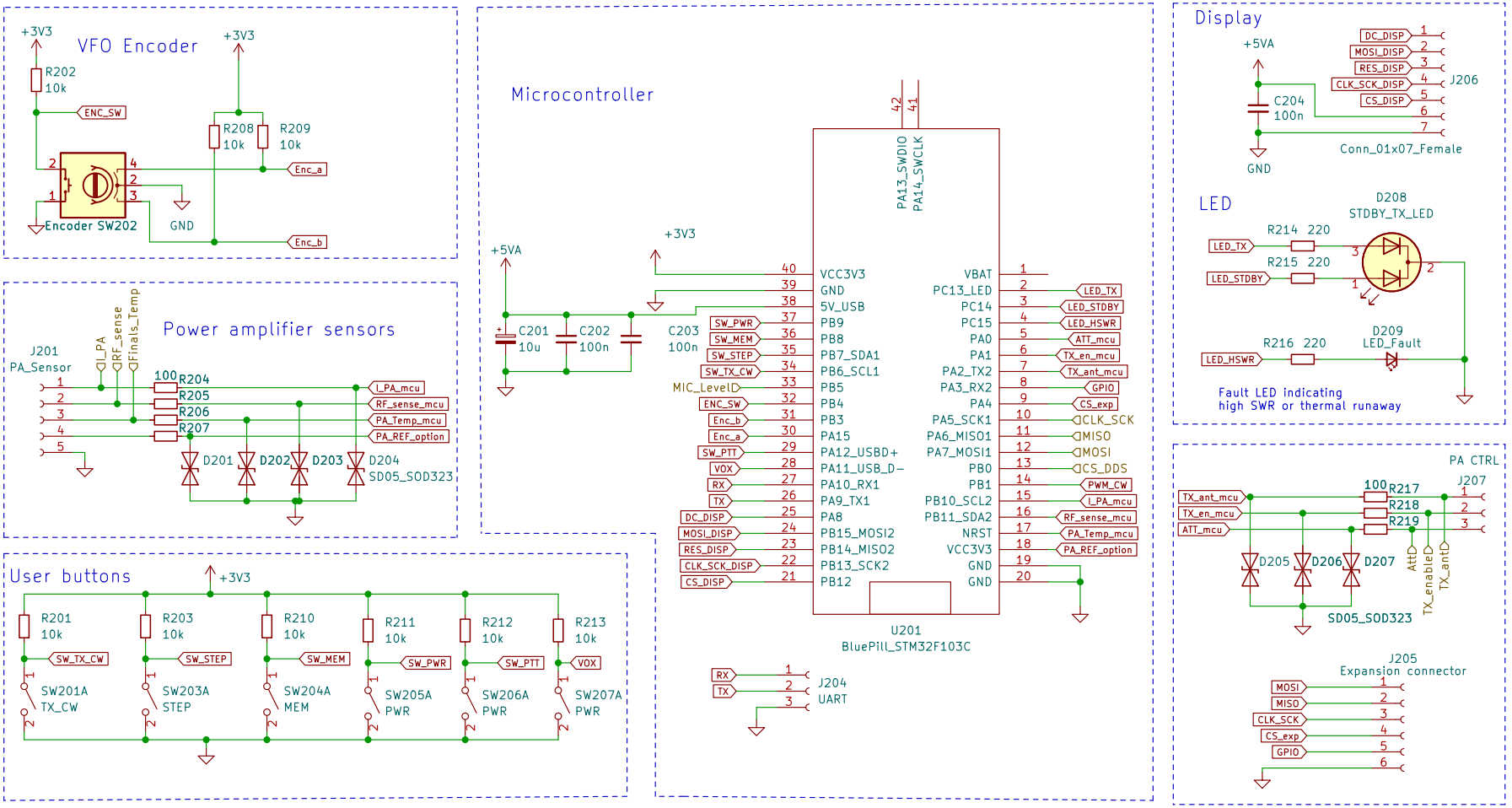


−Encoder, buttons
−LEDs and display connector
−mcu
−Most of front Panel

**Grzegorz Krupa**

Sheet: /Digital/
File: SSB_TX_20m_Digital.kicad_sch

***Title: SSB TX Digital section***

| Size: A4 | Date: 2022−05−09 | **Rev: 1.0** |
|---|---|---|
| KiCad E.D.A. kicad (6.0.9) | | Id: 2/5 |

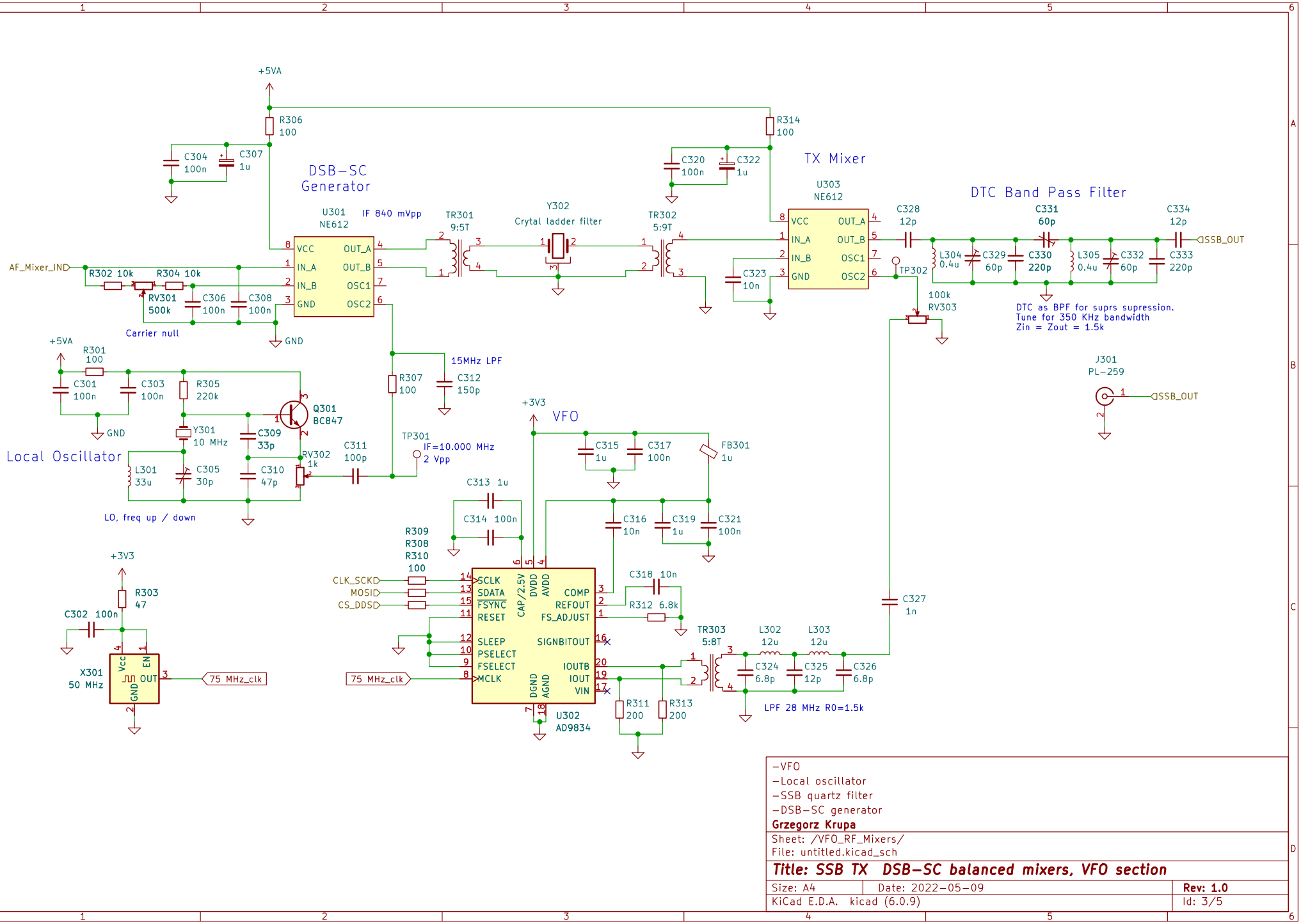


–VFO
–Local oscillator
–SSB quartz filter
–DSB–SC generator

**Grzegorz Krupa**

Sheet: /VFO_RF_Mixers/
File: untitled.kicad_sch

***Title: SSB TX DSB–SC balanced mixers, VFO section***

| Size: A4 | Date: 2022–05–09 | **Rev: 1.0** |
|---|---|---|
| KiCad E.D.A. kicad (6.0.9) | | Id: 3/5 |

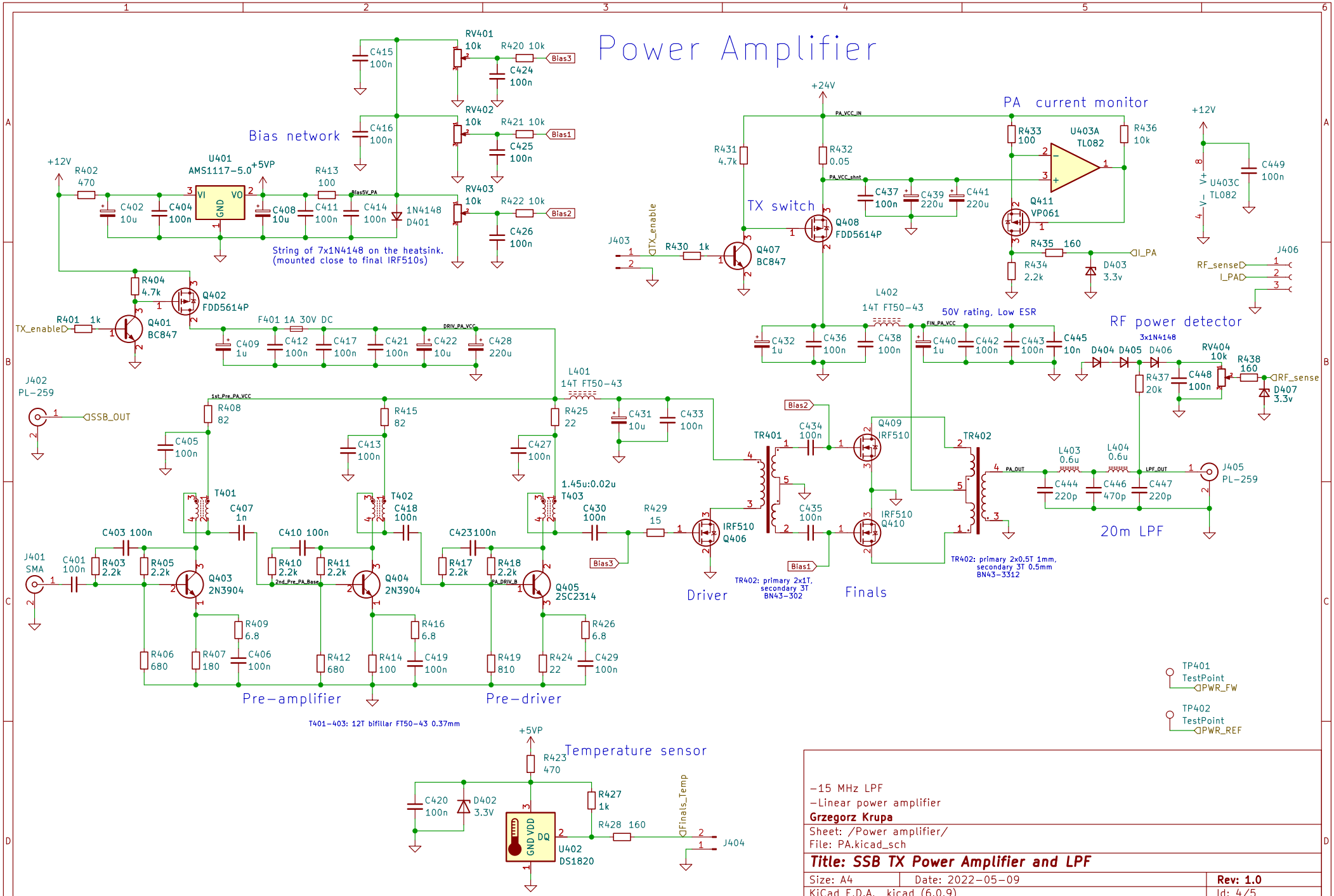
Power Amplifier
Bias network
String of 7x1N4148 on the heatsink.
(mounted close to final IRF510s)
PA current monitor
TX switch
RF power detector
50V rating, Low ESR
Pre−amplifier
Pre−driver
Driver
Finals
20m LPF
Temperature sensor
T401−403: 12T bifilar FT50−43 0.37mm
TR402: primary 2x1T,
secondary 3T
BN43−302
TR402: primary 2x0.5T 1mm,
secondary 3T 0.5mm
BN43−3312
−15 MHz LPF
−Linear power amplifier
Grzegorz Krupa
Sheet: /Power amplifier/
File: PA.kicad_sch
Title: SSB TX Power Amplifier and LPF
Size: A4
Date: 2022−05−09
Rev: 1.0
KiCad E.D.A. kicad (6.0.9)
Id: 4/5

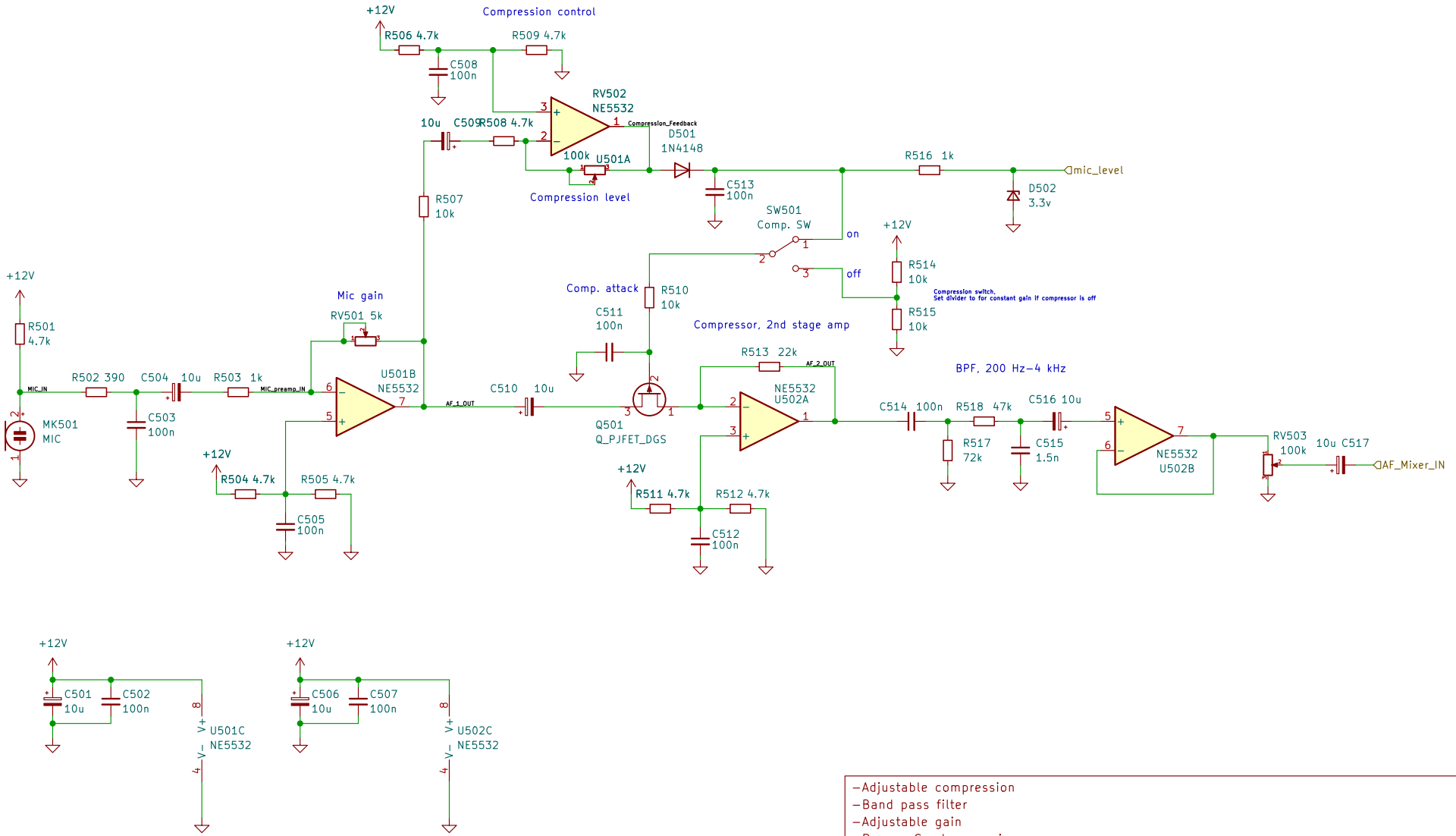


–Adjustable compression
–Band pass filter
–Adjustable gain
–Powers Condenser mic

**Grzegorz Krupa**

Sheet: /Audio/
File: AF.kicad_sch

***Title: SSB TX Audio section***

| Size: A4 | Date: 2022–05–09 | **Rev: 1.0** |
|---|---|---|
| KiCad E.D.A. kicad (6.0.9) | | Id: 5/5 |

# References


[1] D. G. Brown. *Radio and Electronics Cookbook*. Radio Society of Great Britain, 2001.

[2] A. Devoces. Ad9834 rev. d 20 mw power, 2.3 v to 5.5 v, 75 mhz complete dds. 2014.

[3] Eco, Jefferson and Limjoco, Aldrick . Ferrite beads demystified. https://www.analog.com/media/en/analog-dialogue/volume-50/number-1/articles/ferrite-beads-demystified.pdf, 2016. Accessed: 2022-12-14.

[4] Elecraft. Elecraft k3s schematics including options. https://elecraft.com/pages/schematic-files-download-page, 2017. Accessed: 2022-12-07.

[5] Farson, Adam and Austin, Dr.Brian. Ssb compression. https://www.arrl.org/files/file/FCC%20Documents/47%20CFR%20Part%2097%20-%20September%2023%202014.pdf, 2014. Based on an article by Dr. Brian Austin, GØGSF.

[6] W. Hayward, R. Campbell, B. Larkin. *Experimental Methods in RF Design*. ARRL, 2019.

[7] Icom INC. Icom 756 pro ii technical report. https://www.icomamerica.com/en/downloads/DownloadDocument.aspx?Document=26, 2003. ITU classes of emission.

[8] ITU. Crecommendation itu-r bs.640-3. https://www.itu.int/dms_pubrec/itu-r/rec/bs/R-REC-BS.640-3-199710-W!!PDF-E.pdf, 1997. Single sideband (SSB) system for HF broadcasting.

[9] ITU. Telecommunication – updated september 2014. https://www.arrl.org/files/file/FCC%20Documents/47%20CFR%20Part%2097%20-%20September%2023%202014.pdf, 2014. PART 97—AMATEUR RADIO SERVIC, §97.307 Emission standards.

[10] ITU. Commonly notified classes of emission. https://www.itu.int/en/ITU-R/terrestrial/workshops/WRS-16/Documents/Commonly%20notified%20classes%20of%20emission.pdf, 2016. ITU classes of emission.

[11] J. J. Using the ne602. *Electronics Now*, Febuary, 1997.

[12] A. Janeczek. Minitransceiver 80m tinyssb. *Elektronika*, July, 2009.

[13] N. Kennedy. Crystal characterization and crystal filter design. April 26, 2008.

[14] Kitchin, Charles. Avoiding op amp instability problems in single-supply applications. https://www.analog.com/media/en/analog-dialogue/volume-35/number-1/articles/avoiding-op-amp-instability-problems.pdf, 2001. ADI - Contents: Analog Dialogie Volume 35, Number 2.

[15] M. Kossor. A broadband hf amplifier using low-cost power mosfets (part 1). *QST*, March, 1999.

[16] M. Kossor. A broadband hf amplifier using low-cost power mosfets (part 2). *QST*, April, 1999.

[17] R. J. Matthys. *Crystal Oscillator Circuits*, strony 116–119. Krieger Publishing Company, Malabar Florida, 1991.

[18] ON Semiconductors. Mc1496, mc1496b. Access: 08.12.2022 `https://eu.mouser.com/datasheet/2/308/MC1496_D-1773763.pdf`, 2004. Publication Order Number: MC1496/D.

[19] Philips semiconductors. Double-balanced mixer and oscillato ne602. Access: 08.12.2022 `https://www.alldatasheet.com/datasheet-pdf/pdf/107776/PHILIPS/NE602A.html`, 1990. ITU classes of emission.

[20] I. A. Roșu. Bias circuits for rf devices. 2012.

[21] I. A. Roșu. Rf amplifiers. 2012.

[22] R.Smith, Jack. Crystal motional parameters a comparison of measurement approaches. `hhttps://www.mikrocontroller.net/attachment/473317/Crystal_Motional_Parameters.pdf`, 2006. K8ZOA, 11 June.

[23] H. Steder. Crystal ladder filter program "dishal. 2010.

[24] H. Steder, J. A. Hardcastle. Crystal ladder filters for all. *QEX*, November/December:14–18, 2009.

[25] C. Trask. A practical test set for comprehensive crystal testing. 2008.

# Used software and libraries

- KiCad 6.0.9 - EDA software
- FreeCAD 0.20.1 - Parametric 3D modeling software
- LTspice XVII - spice simulation software
- GNU Octave 7.3.0 - Scripts for calculation of circuit parameters
- LibreOffice 7.37.2 - Calc (spreadsheets and graphs), Draw (block diagrams)
- Texmaker 5.1.3 - LaTeX editor
- Dishal - Crytal ladder filter calculator by Horst Steder
- STM32 CubeIDE 1.8.0 - Integrated development environment for STM32 mcu
- STM32 CubeMX - STM32 tool for pin managment
- AD9833 DDS library for STM32 by Analog Devices (Bardia Alikhan Afshar) (modified here for AD9834)

- Mouse bite penalization footprint by Madworm
  $https://github.com/madworm/Panelization.pretty$
- Bluepiill footprint by yet-another-average-hoe
  $https://github.com/yet-another-average-joe/Kicad-STM32$

# List of Figures


1 Designed transmitter . . . . . 1

1.1 Example of AM modulation . . . . . 2
1.2 Block diagram of phase method . . . . . 2
1.3 Block diagram of filter method . . . . . 3
1.4 Ideal case of SSB modulation . . . . . 3
1.5 Block diagram of transmitter . . . . . 4

2.1 Block diagram of AF section . . . . . 5
2.2 Microphone amplifier . . . . . 5
2.3 Schematic of audio compressor . . . . . 6
2.4 Prototype of audio stages . . . . . 6
2.5 Compressor characteristics measured from a prototype . . . . . 6
2.6 AF response characteristics measured from a prototype . . . . . 6
2.7 Schematic of the LO . . . . . 7
2.8 Waveform of LO output . . . . . 7
2.9 Spectrum of the LO . . . . . 7
2.10 Schematic of a Gilbert cell . . . . . 8
2.11 Schematic of NE602 as a balanced mixer . . . . . 8
2.12 Evaluation circuits on copper boards, from left: NE602 mixer, NE602 double balanced mixer, MC1496 double balanced mixer . . . . . 9
2.13 Output from balanced NE602 . . . . . 9
2.14 Spectrum of NE602 output . . . . . 9
2.15 Schematic of balanced mixer with MC1496p . . . . . 10
2.16 Spectrum from MC1496p . . . . . 10
2.17 Model of a crystal . . . . . 11
2.18 Measurement of a crystal . . . . . 11
2.19 Schematic of a 4 crystal ladder filter . . . . . 11
2.20 Crystals divided into smaller batches based on histogram . . . . . 11
2.21 Histogram of examined batch . . . . . 12
2.22 Schematic of modeled crystal and spice test setup . . . . . 12
2.23 Simulation of modeled crystal . . . . . 13
2.24 Dishal filter calculator . . . . . 14
2.25 Spice simulation of filter . . . . . 14
2.26 Spice simulation of a ladder filter with 4 crystals . . . . . 15
2.27 Comparison of 4, 6, 8 crystal filters in LTspice . . . . . 15
2.28 Assembled crystal filter . . . . . 16
2.29 Measurement of passband . . . . . 16

2.30 Wider look at the created filter . . . 16
2.31 Response at the filter output of assembled circuit . . . 17
2.32 SSB output for 1 KHz input signal . . . 17
2.33 Schematic of AD9834 implementation in transmitter . . . 18
2.34 AD9834 with matching transformer and LPF on the PCB . . . 19
2.35 Output of AD9834 with no filter for 14 MHz sine in time domain . . . 19
2.36 Schematic of designed LPF . . . 20
2.37 Simulation of the DDS filter . . . 20
2.38 Singal from the DDS and test of the designed LPF on a real PCB . . . 20
2.39 Diagram of RF mixer . . . 21
2.40 Ideal spectrum that shows up-conversion in a simple way . . . 21
2.41 More complex solution improving sideband rejection . . . 21
2.42 Schematic of TX mixer . . . 21
2.43 Signals from NE602 mixer for different VFO (LO) values and 10 MHz IF . . . 22
2.44 Schematic of double tuned circuit . . . 22
2.45 Assembled DTC . . . 23
2.46 Frequency response output from the exciter . . . 23
2.47 Frequency response output from the exciter . . . 23
2.48 Comparison of Chebyshev and Butterworth DTC in LTspice . . . 24
2.49 Waterfall view of the SSB signal generated by the exciter . . . 24
2.50 Pre-amplifier stage from Lichen transceiver . . . 25
2.51 driver and final stages from lichen transceiver . . . 26
2.52 Low power amplifier . . . 27
2.53 VNA measurement of amplifier's input impedance . . . 27
2.54 Gain for the IRF510 single ended amplifier, test of assembled circuit . . . 27
2.55 Schematic of final stage . . . 28
2.56 Bias network for the finals . . . 28
2.57 Signal flow through a push pull MOSFET amplifier simulated in LTspice . . . 29
2.58 Simulation of final stage . . . 29
2.59 Assembled final stage . . . 29
2.60 LPF test with VNA . . . 30
2.61 LPF test with SA . . . 30
2.62 Dummy load . . . 31
2.63 Output of PA without LPF . . . 31
2.64 Output of PA with LPF . . . 31
2.65 Gain chart for the assembled amplifier . . . 32
2.66 Compression point and linearity chart . . . 32
2.67 Temperature of finals over time . . . 33
2.68 DC power draw for given RF output . . . 33
2.69 Efficiency vs output power . . . 33
2.70 Antenna relay circuit . . . 33

3.1 Device is split into two boards that can be penalized. . . . 34
3.2 8 crystals version of SSB filter . . . 34
3.3 Assembled exciter PCB, only prototype revision was assembled . . . 35
3.4 PCB assembly diagram . . . 35
3.5 Front of the transmitter . . . 35
3.6 Transmitter during assembly . . . 35

# List of Tables

2.1 Characteristic of Spice simulated crystal from G3UUR method for a real crystal tested using spectrum analyzer . . . . . 13
2.2 Measurements for two methods of evaluating the motional parameters of crystal resonator with results. Colors correspond to method used and data gathered for that method. . . . . 14
2.3 Steepness of upper and lower slope of ladder filter with n crystals (according to a simulation based on measured motional parameters of generic 10 MHz crystal) . . 15